T.R.

GEBZE TECHNICAL UNIVERSITY

GRADUATE SCHOOL OF NATURAL AND APPLIED SCIENCES

NUMERICAL ANALYSIS OF HEADER RELATED FLOW MALDISTRIBUTIONS ON MICRO CHANNEL HEAT EXCHANGERS USING ANISOTROPIC POROUS MEDIA APPROXIMATION

ALİ ELMALI

A THESIS SUBMITTED FOR THE DEGREEE OF

MASTER OF SCIENCE

DEPARTMENT OF MECHANICAL ENGINEERING

GEBZE

2019

T.R.
GEBZE TECHNICAL UNIVERSITY
GRADUATE SCHOOL OF NATURAL AND APPLIED SCIENCES

NUMERICAL ANALYSIS OF HEADER RELATED FLOW MALDISTRIBUTIONS ON MICRO CHANNEL HEAT EXCHANGERS USING ANISOTROPIC POROUS MEDIA APPROXIMATION

ALİ ELMALI

A THESIS SUBMITTED FOR THE DEGREEE OF
MASTER OF SCIENCE
DEPARTMENT OF MECHANICAL ENGINEERING

THESIS SUPERVISOR
ASSOC. PROF. DR. MUSTAFA FAZIL SERİNCAN

GEBZE
2019

T.C.
GEBZE TEKNİK ÜNİVERSİTESİ
FEN BİLİMLERİ ENSTİTÜSÜ

MİKROKANALLI ISI DEĞİŞTİRİCİLERİNDE BAŞLIK KAYNAKLI AKIŞ DÜZENSİZLİKLERİNİN ANİZOTROPİK POROZ ORTAM YAKLAŞIMI KULLANARAK NUMERİK ANALİZİ

ALİ ELMALI
YÜKSEK LİSANS TEZİ
MAKİNE MÜHENDİSLİĞİ ANABİLİM DALI

DANIŞMANI
DOC. DR. MUSTAFA FAZIL SERİNCAN

GEBZE
2019

GEBZE TEKNİK ÜNİVERSİTESİ	**YÜKSEK LİSANS JÜRİ ONAY FORMU**

GTÜ Fen Bilimleri Enstitüsü Yönetim Kurulu'nun ..10../..07../..2019 tarih ve .2019../.....31.. sayılı kararıyla oluşturulan jüri tarafından ..29../..07../..2019 tarihinde tez savunma sınavı yapılan Ali ELMALI 'ın tez çalışması Makine Mühendisliği Anabilim Dalında YÜKSEK LİSANS tezi olarak kabul edilmiştir.

JÜRİ

ÜYE
(TEZ DANIŞMANI) : DOC. DR. MUSTAFA FAZIL SERİNCAN

ÜYE : PROF. DR. FEVZİ BEDİR

ÜYE : PROF. DR. BURAK DİKİCİ

ONAY

Gebze Teknik Üniversitesi Fen Bilimleri Enstitüsü Yönetim Kurulu'nun
...../...../..... tarih ve ...../..... sayılı kararı.

SUMMARY

Microchannel heat exchangers have been used extensively in applications where high heat rejection rates are needed in restricted places. Providing a uniform flow distribution at the inlet of the microchannels plays a crucial role in the efficiency of the heat exchanger. Uneven flow distribution across the microchannels is one of the main concerns leading to uneven heat transfer across the surfaces. Moreover, micro channel heat exchangers are not practically easy to produce devices in case when they are intended to be used in experimental analyses and performance measurements. This situation makes it mandatory to use numerical methods to test and take performance measurements from heat exchangers. Despite the fact that modern computer technology gives the opportunity of having high amount of processing power, the complex structure and high number of elements used in heat exchanger analysis make these computations rather difficult and time consuming. In this case, either a small part of the heat exchanger is analyzed or whole 3D body has to be analyzed. With these problems in mind, usability of porous media approximation in 3D model analyses is validated. Performances of 3D and porous approximated models in terms of computation time and load are compared. A maldistribution on a microchannel is analyzed using porous media approximation for the sake of simplicity and to reduce time. Fluid flow and the heat transfer across the microchannel is investigated. Based on the model results, some design guidelines for the header and channel inlet cross-sections are recommended.

Key Words: Anisotropy, CFD, Heat exchanger, Maldistribution, Microchannel, Porosity

ÖZET

Mikro kanallı ısı değiştiricileri özellikle kısıtlı alanlarda yüksek ısı transfer oranlarının istendiği yerlerde geniş kullanım alanlarına sahiptir. Mikrokanallı ısı değiştiricilerinden en üst düzeyde verim elde edebilmek için akışın eşit dağıtılması önemli bir rol oynar. Kanallarda oluşan eşit olmayan akış dağılımları aynı şekilde eşit olmayan ısıl dağılımlarına neden olmaktadır. Ayrıca mikro kanallı ısı değiştiricileri üretimlerinin çok pratik olmaması sebebiyle deneysel olarak test etmek ve performans ölçümleri yapmak açısından kullanışlı araçlar değillerdir. Bu durum mikro kanalların test edilmeleri ve performans ölçümleri için numerik analizlerin kullanılmalarını daha zorunlu hale getirmiştir. Ancak mikro kanalların küçük ve karmaşık yapıları nedeniyle günümüz de kullanabildiğimiz yüksek kapasiteli bilgisayarlar için bile bu büyük bir işlem gücü demektir. Bu durumda ya mikro kanalın küçük bir kısmı incelenir ya da uzun süren işlemler neticesinde tüm gövde analiz edilir. İlk durum zaman ve işlem tasarrufu sağlasa da tüm gövde analiz edilemediği için tüm gövde analiz edildiğinde elde edilen bilgiyi vermez. İkinci durum ise büyük zaman ve işlem gücü gerektirir. Bu durumlar göz önüne alınarak poroz ortam yaklaşımının 3D kanalları modellemede kullanılabilirliği valide edilmiştir. Poroz ortam yaklaşımı ile 3D analiz arasında performans kıyaslaması yapılmıştır. Bununla birlikte poroz ortam yaklaşımı kullanılarak su girişi tarafında oluşan başlık kaynaklı akış düzensizliklerinin HAD (Hesaplamalı Akışkanlar Dinamiği) analizleri yapılmış ve incelenmiştir. Akış düzensizliklerini en aza indirmek için tasarım önerileri verilmiştir.

Anahtar Kelimeler: Anizotropi, HAD, Isı Değiştiricisi, Mikro Kanal, Porozite

ACKNOWLEDGEMENTS

I wish to express my sincere gratitude to my supervisor, Assoc. Prof. Dr. Mustafa Fazıl SERİNCAN for his supports in scope of this study.

I am grateful to my mother, sister and cousin for their love and support.

Finally, I want to thank Esra KOÇ, who showed me the beauty of love and BİRGİ A.Ş. workers for their immortal friendship

TABLE OF CONTENTS

	Page
SUMMARY	iv
ÖZET	v
ACKNOWLEDGEMENTS	vii
CONTENTS	vii
LIST OF ABBREVATIONS AND ACRONYMS	x
LIST OF FIGURES	xi
LIST OF TABLES	xii
1. INTRODUCTION	1
1.1. The Literature Review	3
1.2. Outline of the Study	6
2. VALIDATION OF POROUS MEDIA APPROXIMATION	6
2.1. Description of Problem	6
2.2. Porous Model	10
2.3. Anisotropic Permeability	11
2.4. Structure of the Mesh	12
2.5. Mesh Dependency	13
3. VALIDATION RESULTS	14
3.1. Comparisons of Temperature Changes Across a Single Channel	15
3.2. Heat Gradients Over Whole Body	18
3.3. Symmetry Plane Heat Gradients	19
3.4. Vertical plane heat gradients	22
3.5. Pressure Drop	25
3.6. Computation Time	26
4. MALDISTRIBUTION	27
4.1. Mathematical Models	28
4.2. Manifold Related Flow Maldistribution Scenarios	30
4.2.1. Scenario 1	30

4.2.2. Scenario 2 31
4.2.3. Scenario 3 32
4.3. Randomly Occurred Maldistribution Scenarios 33
4.3.1. Scenario 4 33
4.3.2. Scenario 5 34
4.4. Analysis Results 35
4.4.1. Scenario 1 35
4.4.2. Scenario 2 37
4.4.3. Scenario 3 38
4.4.4. Scenario 4 40
4.4.5. Scenario 5 41
4.5. Discussion About Maldistribution 42
5. GENERAL DISCUSSION 43

REFERENCES 49
BIOGRAPHY 52

LIST OF ABBREVATIONS AND ACRONYMS

Abbreviations and Acronyms		**Explanations**
ρ	:	Density
u	:	Velocity
∇	:	Delta operator
c_p	:	Heat capacity at constant pressure
μ	:	Dynamic Viscosity
k	:	Thermal Conductivity
$\dot{m}_{input}$	:	Mass flow rate
Q_{heat}	:	Heat source power
T_{input}	:	Input temperature of water
κ	:	Permeability
ε	:	Porosity
W_{chn}	:	Channel Width
W_{fin}	:	Fin Width
CFD	:	Computational Fluid Dynamic
MHE	:	Microchannel heat exchanger
PDE	:	Partial differential equation

LIST OF FIGURES

Figure No: **Page**

2.1: Half and full view of microchannel heat exchanger used in numerical analysis. 7

2.2: Microchannel dimensions. 8

2.3: Porous model. 11

2.4: Mesh structures of porous and 3D models. 12

2.5: Mesh structure showing boundary layers. 13

3.1: Data line probe for acquiring temperature data from the location of the line. 15

3.2: from left to right 20 and 30 um 3D and porous model temperature curves taken from data line in Figure 6. 15

3.3: from left to right 40 and 60 um 3D and porous model temperature curves taken from data line in Figure 6. 16

3.4: From left to right 90 and 180 um 3D and porous model temperature curves taken from data line in Figure 6. 16

3.5 : Overall temperature curves for porous models. 17

3.6: Overall temperature curves for 3D models. 17

3.7: Total view of temperature curves of 3D and porous models. 18

3.8: Symmetry and vertical data planes which supply temperature data for heat gradients on symmetry plane. 19

3.9: 20 um micro channel heat gradient of 3D and porous models on symmetry plane. 20

3.10: 30 um micro channel heat gradient of 3D and porous models on symmetry plane. 20

3.11: 40 um micro channel heat gradient of 3D and porous models on symmetry plane. 21

3.12: 60 um micro channel heat gradient of 3D and porous models on symmetry plane. 21

3.13: 90 um micro channel heat gradient of 3D and porous models on symmetry plane. 22

3.14: 180 um micro channel heat gradient of 3D and porous models on symmetry plane. 22

3.15: 20 um micro channel heat gradient of 3D and porous models on vertical plane. 23

3.16: 30 um micro channel heat gradient of 3D and porous models on vertical plane. 23

3.17: 40 um micro channel heat gradient of 3D and porous models on vertical plane. 24

3.18: 60 um micro channel heat gradient of 3D and porous models on vertical plane. 24

3.19: 90 um micro channel heat gradient of 3D and porous models on vertical plane. 25

3.20: 180 um micro channel heat gradient of 3D and porous models on vertical plane. 25

3.21: Pressure drops across the data line shown in Figure 6. 26
4.1: Scenario 1 header model and flow direction. 30
4.2: Velocity curve at the inlet for scenario 1. 31
4.3: Scenario 2 header model and flow direction. 31
4.4: Velocity curve at the inlet for scenario 2. 32
4.5: Scenario 3 header model and flow direction. 32
4.6: Velocity curve at the inlet for scenario 3. 33
4.7: Velocity curve at the inlet for scenario 4. 34
4.8: Velocity curve at the inlet for scenario 5. 35
4.9: Overall temperature gradient of scenario 1 and velocity distribution across symmetry plane 36
4.10. Outlet temperature of the model in scenario 1. 36
4.11: Overall temperature gradient of scenario 2 and velocity distribution across the symmetry plane 37
4.12.: Outlet temperature of the model in scenario 2. 38
4.13: Overall temperature gradient of scenario 3 and velocity distribution across symmetry plane. 39
4.14. Outlet temperature of the model in scenario 3. 39
4.15: Overall temperature gradient of scenario 4 and velocity distribution across symmetry plane. 40
4.16. Outlet temperature of the model in scenario 4. 40
4.17: Overall temperature gradient of scenario 5 and velocity distribution across symmetry plane. 41
4.18. Outlet temperature of the model in scenario 5. 42

LIST OF TABLES

Table No:		Page
2.1:	Properties of materials used.	7
2.2:	Channel widths and number of channels of the models.	8
2.3:	Boundary condition values of the models.	9
2.4:	Porosity and permeability values of porous models.	10
2.5:	Number of elements used in 3D and porous models.	13
2.6:	Change in the outlet temperatures with respect to change in number of elements in a single model.	14
3.1:	Computation times of 3D and porous models.	27
4.1:	Output values of the model in scenario 1.	37
4.2:	Output values of the model in scenario 2.	38
4.3:	Output values of the model in scenario 3.	39
4.4:	Output values of the model in scenario 4.	41
4.5:	Output values of the model in scenario 5.	42

1 INTRODUCTION

Today's electronic devices are expected to be very fast, compact in order to meet today's requirements. For an electronic device to go in to faster working speeds, special integrated circuits are designed but the faster a device is, the more energy that device is consuming and produces more heat. This excess heat also plays a major role reducing the efficiency of these devices. Also, compactness in a device requires its elements to be rather small. Generally, to dissipate high heat loads requires wide heat transfer areas. But using high volume equipment in devices make it impossible to build compact devices. In order to solve this problem, a small and effective solution was needed.

Conventional air-cooled heat exchangers are proven to be not sufficient to dissipate heat loads of 500 W/cm^2 and above from devices like CPU, GPU and power amplifiers that have limited space for cooling. These conventional methods often require high flow velocities to dissipate such high heat loads. High velocities usually associate with noise and vibration problems. This situation forced many researchers to find new possible ways to efficiently cool down equipment that generates high heat loads. Thus, many researchers lead their ways to find more innovative heat exchanger models like heat pipes, heat chambers, nanomaterials, fluid coolant systems and miniature systems. Absolute goal here is to reduce heat resistance between the medium and heat generating device and keep temperature of the surface of the device as possible.

Idea of using microchannel heat exchangers which is one of these innovative ideas was first proposed in 1984 [1]. According to the proposed idea, the fluid is forced through a set of narrow passages which are called micro channel and thus, total heat transfer area is increased. This way, devices that requires a limited volume for heat transfer can be cooled down efficiently.

Heat exchangers with microchannel flow ways are becoming popular because of their ability to remove large heat loads under single-phase and two-phase applications like aerospace, automotive, bioengineering, cooling of gas turbine blades, power and process industries, refrigeration and air conditioning, infrared detectors and powerful laser mirrors and superconductors, microelectronics, and thermal control of film deposition. The one of the most important advantages of microchannel heat exchangers

are high volumetric heat flux, compactness for low space applications, robust design, effective flow distribution, and good pressure drops.

As in the other heat transfer devices, there are some factor that effects the efficiency of the device in negative ways. One of the most crucial of them is the case when the fluid is not evenly distributed to the channels. This phenomenon is called maldistribution. Maldistribution means that the heat transfer is not evenly done by all channels. One of the major factors that causes this problem is manifold design which is the first element in heat exchangers that touches the flow and is meant to distribute it. But not every design is so successful in evenly distribution. Other factor is flow medium related problems like particles inside the fluid which can clog the channels and cause fouling. Flow maldistributions can also cause device to overheat and broke down beside the reduction in efficiency.

Analyzing the flow maldistribution using CFD can give information about possible manifold and channel designs. However, making a CFD maldistribution analysis in a 3D whole model requires lots of time and computer processing loads. It is not nearly possible to analyze whole body using todays modern computers. The reason for this is that meshing whole 3D model produces many elements that is beyond computers' processing and memory power. Even if it is possible to solve CFD codes of whole 3D model, since it takes lots of times, the analyzer would live difficulties when there was an error after an analysis. Because of these reasons, researchers take one or two channels and analyze it and uses the acquired information for whole model. This is quite improper when one needs to see what is happening in whole model.

All these studies that are about maldistribution and other topics which needs CFD were made using conventional CFD codes. Even it is possible, meshing and computing whole 3D model using these codes costs lots of computational power and time. Also, these methods are usually applied to a small part of the model and are hard to apply to complex models. This is not a realistic approach to problems.

In the middle of the 80's, the microchannel models was modelled as porous medium using Darcy law [2]. According to the proposed method, the micro channel domain is modelled as porous medium and a relationship is set between the material properties of the porous medium and geometric parameters of the channels. By this way, a complex set of micro channel domain is reduced to a single domain. After, whole model can be meshed and solved easily. This method later was applied [29] and

extended [4] to calculate heat and velocity distribution in micro channel heat exchangers as volume averaged approach.

1.1 The Literature Review

In literature, the heat exchangers with channel width 3mm and above is macro, channel width between 200 um and 3 mm is mini channel and lastly the channel width between 1 um and 200um is regarded as micro channel [8]. However, the term micro channel is used for the heat exchanger that has hydrolytic diameter higher than 200 um.

In practice, small flow rate inside the microchannels result in laminar flow which cause heat transfer coefficient inverse proportional to hydraulic diameter. Namely, the narrower the channel, the higher the heat transfer coefficient is.

In literature, the application of fluids like air and pure water in microchannels is experimented. When the studies that was conducted since 80's is investigated, there were researches about heat and flow analysis on microchannels. Despite there are a number of researches like these. It can not be said that there is enough application analysis of these devices.

A critical review was written which presents a compilation and analysis of the results from investigations on fluid flow and heat transfer in micro and mini channels and microtubes in the literature up to 2000 [22]. They concluded "Given the diversity in the results in the literature, a reliable prediction of the heat transfer rates and pressure drops in microchannels is not currently possible for design applications such as microchannel heat sinks."

Another critical review which explores the recent developments like pool boiling, detachable heat sinks, channel flow boiling and micro and mini channel heat exchangers in high rate thermal management is written [27].

Microchannel heat exchangers is used to extract high heat loads from laser diodes that generates heat flux up to 500 W/cm^2. They forced water through the channels located within a few hundred micrometers of active devices fabricated on the surface of semiconductor wafers. They used silicone as heat exchanger material and manufactured the channels using a dicing saw. They choose the silicone because it has a high thermal conductivity and it is easy to machine. the velocity through the channels is near transition since the Reynold was reached to 2000 [26].

High-performance air-cooling scheme was theoretically and experimentally invertigated using micro channel parallel plate-fin heat exchanger and tubes to deliver the air to. They modelled the performance of exchangers in terms of thermal resistance, pumping power and pressure drop. They made some optimization on and gave some guideline for the design [5].

A comparative investigation of jet impingement and microchannel cooling was made. They revealed that micro channel cooling is good for the application spaces of 0.07 m x 0.07 m [24].

Different type of heat transfer devices including microchannel heat exchangers was compared [6].

Theorical and numerical studies investigating classical single layer microchannels was made. They solved numerically a conjugate heat transfer problem and presented an algorithm for the selection of the heat exchangers dimensions [16].

According to a critical review on numerical and experimental analyses on this matter, further studies are required to generate a sufficient body of knowledge of the transport mechanism responsible for the variation of the flow structure and heat transfer in microchannels [15].

A review which critically evaluates experimental setups and data acquisition techniques was written and various aspects such as entrance region effects, channel dimension effects, boundary conditions etc was reviewed .

In an experiments on the heat exchanger which was manufactured using additive manufacturing method, they designed air passages as tapered manifolds so as to force the inlet air through the microchannels and collect the air at the outlet. With this, they aimed to cool down cross flowing water [17]

As in the other heat transfer devices, there are some factor that effects the efficiency of the device in negative ways. One of the most crucial of them is the case when the fluid is not evenly distributed to the channels. This phenomenon is called maldistribution. Maldistribution means that the heat transfer is not evenly done by all channels. The importance of this problem has led researchers to study the effect of the maldistribution and led them to seek alternative manifold designs and flow medium improvements.

For example, according to an experimental analysis on flow maldistribution in microchannels with 25 channel using different type of manifold design, it was concluded that trapezoidal header gives less flow maldistribution.

In an experimental analysis inwhich basic parameters in microchannels such as number of channels, area of cross section of the manifold, channel hydraulic diameter, and Reynolds numbervaries. It is resulted that reducing hydraulic diameter in micro channels considerably reduces flow maldistribution. They also pointed out that the change in Reynold number doesn't have great importance on maldistribution. They also found with the increasing number of channels the flow maldistribution also increases [25].

Double inlet header design is proposed to reduce effect of flow maldistribution by mitigating it. The flow rate maldistribution is reduced by about 68.5% and micro channel efficiency is improved by 7.7% [28].

Numerical simulations was made to study flow maldistribution in a U-type micro channel. They showed that increase in flow resistance by decrease in channel depth, width or number of channels or increase in channel length, results in a more uniform distribution. they also showed that Mal-distribution increases at high flow rate or low viscosity due to the dominance of inertial effects [23].

All these studies that are about maldistribution and other topics which needs CFD were made using conventional CFD codes. Even it is possible, meshing and computing whole 3D model using these codes costs lots of computational power and time. Also, these methods are usually applied to a small part of the model and are hard to apply to complex models. This is not a realistic approach to problems.

In the middle of the 80's, microchannel heat exchanger was modelled the as porous medium using Darcy law [2]. They created a physical model that the micro channel domain is substituted by a porous domain and they assumed heat flux is removed by a passing coolant at a flow rate through the porous medium material in the channel. their main purpose is to calculate temperature distribution in porous material (microstructures) and the coolant. This method later was applied [29] and velocity and temperature distributions through microchannel heat sinks was presented by modeling the microchannel heat sink as a fluid-saturated porous medium. They extended this method by using volume averaging approach for the velocity and temperature distribution in microchannel [4].

1.2 Outline of the Study

CFD analysis of flow maldistribution in micro channels takes a lot of time since 3D model contains lots of elements. With this fact in mind, a micro channel is modelled as porous approximated model and different type of flow maldistribution scenarios are created to examine the effects of flow maldistributions in micro channels. the input velocity profiles for each scenario are defined by particular mathematical models that are highly possible to occur in real cases. As previously stated, to reduce computation time and load, models are analyzed by using porous medium approach.

Before using porous medium approach in maldistribution analysis, validation of this method was made. Also, the usage limits of the method are calculated. To do that, heat gradients on 3D modelled 6 heat exchangers which are modelled with 6 different channel number are compared with their porous domain matches and acquired results are presented and interpreted.

The dimensions of the models are taken from the model which is previously used in a study [17]. After validating the porous media approximation, the method is used to simulate the flow maldistribution across a microchannel with 60 um channel width. Acquired results are interpreted and used for giving some sdesign advices.

2 VALIDATION OF POROUS MEDIA APPROXIMATION

2.1 Description of Problem

In this study, a micro channel heat exchanger is used to cool down a heat source. Water is used as cooling fluid and it passes through the microchannels. The heat which is intented to be taken away presented as a constant heat flux just underneath the exchanger. The amount of heat to dissipate is $1W/mm^2$. Outer dimensions and channel dimensions are taken from the model which is previously used in a study [17]. The dimensions, images and whole model image can be seen in Figure 2.1. Also, a detailed view of the 3D model can be seen in Figure 2.2

Half of the whole geometry is used in analysis so as to simplify the analysis. To do that, a symmetry boundary condition is used on the upper surface of the model. By

using symmetries in a model, its size can be reduced by one-half or more, making this an efficient tool for solving large problems. This applies to the cases where the geometries and modeling assumptions include symmetries.

The material which is used as solid domain material is stainless steel and fluid domain material is water. In Table 2.1, the properties of the materials used in the study can be seen.

Table 2.1: Properties of materials used

Name of the materials	**Thermal Conductivity (W/m.K)**	**Density (Kg/m^3)**	**Heat capacity at constant pressure (J/kg.K)**
Stainless Steel	15	7800	420
Water	0.606	1000	4180

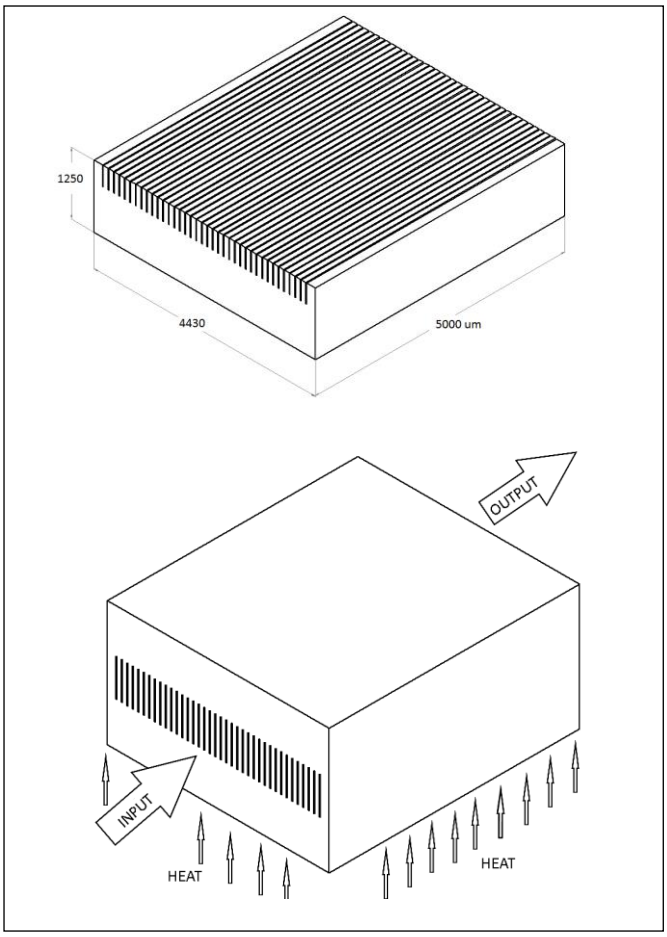

Figure 2.1 Half and full view of microchannel heat exchanger used in numerical analysis

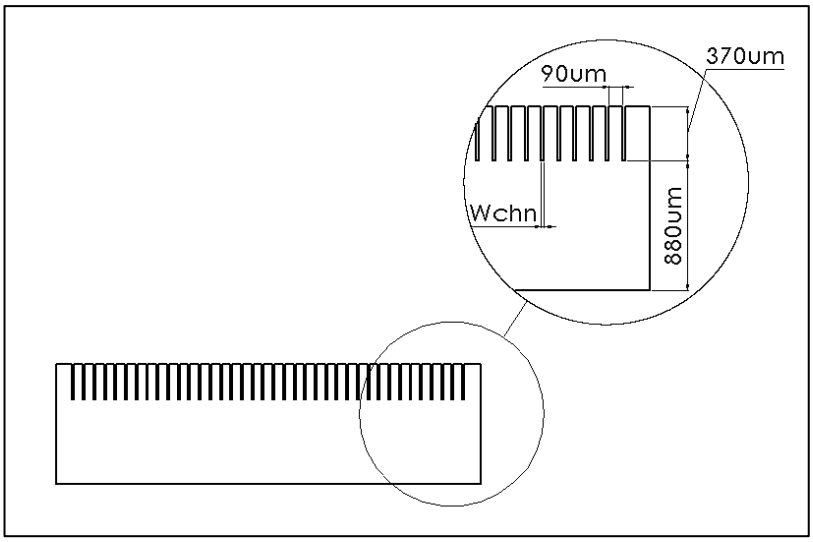

Figure 2.2 Microchannel dimensions

To validate that desired results are not changing when geometric parameters change, different types of microchannel models with different size of channel widths are used and analysed. Similarly, porous media approximated matches of the considered 3D models are also analysed. 6 different type of channel size are used. Channel width of these models are defined as to be 20, 30, 40, 60, 90, 180um. The outer dimensions of all models, as seen in Figure 1 and 2, kept same for all models. As a result of this, with the changing channel sizes, the number of the channel is also changed. The number of channels corresponding to channel sizes are presented in Table 2.2.

Table 2.2 Channel widths and number of channels of the models

Channel Width (Wchn(um))	**Number of Channel (n)**
20	38
30	35
40	33
60	28
90	24
180	16

Here, water is assumed to be incompressible fluid. Also, it is assumed to fully developed and single-phased. Steady state governing equations are;

Mass:

$$\rho\nabla.(u)=0 \tag{2.1}$$

Momentum:

$$\rho(u\nabla)u= \nabla.[-\rho\imath+K]+F \quad (2.2)$$

$$K= \mu(\nabla u+(\nabla u)T) \quad (2.3)$$

Energy:

$$\rho cpu.\nabla T+\nabla.q=Q \quad (2.4)$$

$$q=-k\nabla T \quad (2.5)$$

These equations for 3D models are solved using COMSOL Multiphysics software which uses finite elements method.

Similarly, for the porous model, equations below are solved;

Mass:

$$\rho\nabla.(u)=Qm \quad (2.6)$$

Momentum:

$$\frac{1}{\varepsilon_p}\rho(u.\nabla)u\frac{1}{\varepsilon_p} = \nabla[-p\imath + \mu\frac{1}{\varepsilon_p}\left(\nabla u + (\nabla u)^T\right) - \frac{2}{3}\mu\frac{1}{\varepsilon_p}(\nabla.u)\imath\Big] - \left(\mu\kappa^{-1} + \beta_F|u| + \frac{Q_m}{\varepsilon_p^2}\right)u + F \quad (2.7)$$

Energy:

$$\rho cpu.\nabla T+\nabla.q=Q \quad (2.8)$$

$$q=-k\nabla T \quad (2.9)$$

The boundary conditions are listed in Table 2.3 below.

Table 2.3 Boundary condition values of the models

T_{input}(K)	$\dot{m}_{input}$(kg/s)	Q_{heat}(W/mm^2)
300	5e-5	1

To make an approximation for a 3D model, there must be some other equations which defines a relation between the geometric parameters of 3D models and porous medium properties of the porous models. These porous medium properties are porosity and permeability which are ratio of volume of gaps to whole volume and ability to transmit fluid through the porous domain respectively. At this point, a set of special equations 2.10 and 2.11 which is proposed before is used [4]. These are;

$$\varepsilon = \frac{W_{chn}}{W_{chn} + W_{fin}} \tag{2.10}$$

$$\kappa = \frac{\varepsilon . W_{chn}^2}{12} \tag{2.11}$$

According to the equations proposed [4], porosity is a function of channel width and fin width. Similarly, permeability is a function of the porosity which is obtained and channel width. With the help of these equations, porosity and permeability values for each size of models are calculated. Porosity and permeability values corresponding to the channel sizes are listed in Table 2.4.

Table 2.4 Porosity and permeability values of porous models

Channel Widths (um)	**Porosity (ε)**	**Permeability (κ)**
20	0.18	6.06e-12
30	0.25	1.87e-11
40	0.31	4.1e-11
60	0.4	1.2e-10
90	0.5	3.375e-10
180	0.66	1.8e-9

In the light of these information porosity and permeability values listed are used as a material property values for porous domain.

2.2 Porous Model

The outer dimensions of the porous models are kept same with 3D models. In porous models, the area of the channels in 3D models are described as a single porous domain in porous models. An image which shows porous model is shown in Figure 3. The porosity and permeability values of this domain is assigned according to the values in Table 2.4. Thus, for each different type of 3D models, there created a porous model with different porosity and permeability values.

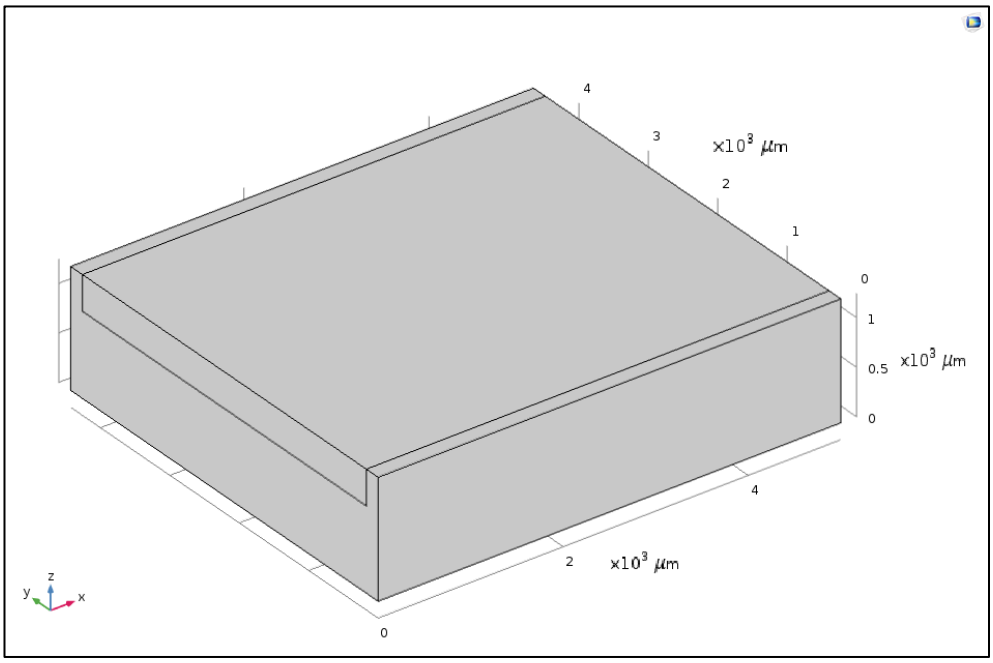

Figure 2.3 Porous model

2.3 Anisotropic Permeability

Anisotropy means that some properties of the porous medium do not have the same value in different directions. In an anisotropic porous medium, the permeability, formation resistivity factor, and breakthrough capillary pressure depend on the direction. In the most general case these properties are function of both location in the medium and orientation. Thus the probability density function for each property can be described with five independent variables (x, y, z) for location and (θ,φ) for orientation. If the probability density distribution is independent of the angular coordinates, the medium is isotropic, otherwise it is anisotropic.

The porous domain created can be expressed with tensors. In other words, permeability has a direction feature. With the help of this feature, the direction of the flow in 3D model can be mimicked by using tensor feature of the permeability property of porous domain. The tensor is regarded as diagonal and permeability values in the directions except the direction which the fluid flow toward is entered a value which is close to zero. By doing this, fluid flow to the other directions except the direction the fluid flows through is blocked. In conclusion, 3D models are fully represented as

porous medium which has a flow direction. In 2.12, tensor input for channel of size 20 um can be seen.

$$\begin{bmatrix} \kappa & 0 & 0 \\ 0 & 10e-23 & 0 \\ 0 & 0 & 10e-23 \end{bmatrix} \tag{2.12}$$

The boundary condition which is applied to the porous model is exactly same as 3D models. Thus, both type of model is investigated under equal circumstances. As in 3D models, symmetry boundary condition is applied to porous models.

2.4 Structure of the Mesh

To obtain proper results in fluid dynamic problems, it is advisable to use quad meshes. In both types of models, porous and 3D, the input side surfaces of the models are quad mapped and that mapped surfaces are swept along the model length. That procedure created a uniform layer of quadratic meshes. Mesh structures of both porous and 3D models can be seen In Figure 2.4 and 2.5.

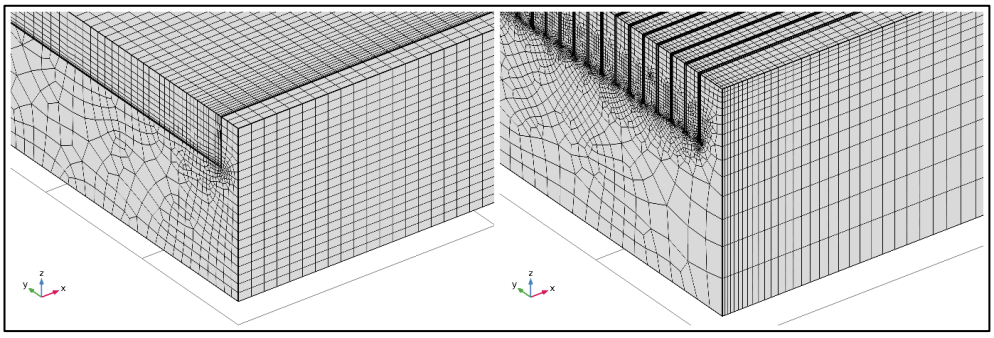

Figure 2.4: Mesh structures of porous and 3D models

To see the velocity gradient and effects of no slip conditions across the boundaries, boundary layers are applied, Figure 2.5.

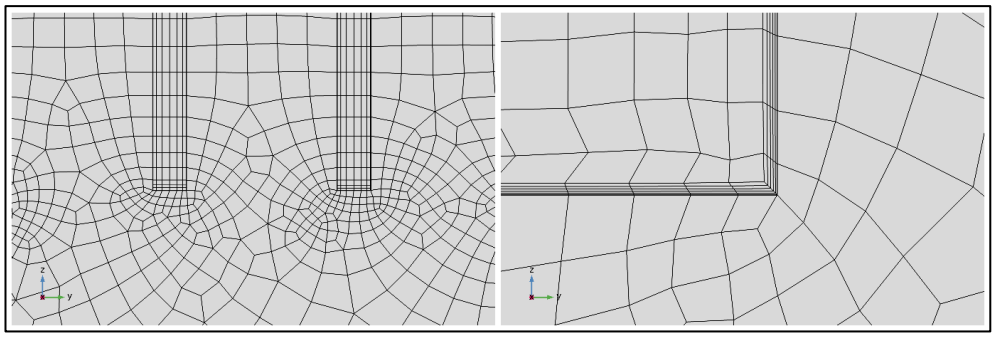

Figure 2.5: Mesh structure showing boundary layers

Coarser mesh is used at the areas other than the fluid domains since these solid areas don't need fine meshes.

Therefore, the number of elements that are used in 3D and porous models are listed in Table 2.5.

Table 2.5: Number of elements used in 3D and porous models

Channel Width (um)	3D Model	Porous Model
20	1131600	110200
30	978000	112450
40	897840	107450
60	756480	112450
90	644960	111800
180	575840	111800

2.5 Mesh Dependency

The term mesh dependency is an important factor when solving CFD problems. Mesh structures need to be developed to eradicate mesh dependency without compromising the finite computing resource and/or incurring large computational expense. In deciding upon an acceptable mesh structure, a compromise should be sought between high computational accuracy, short solution-time and cost-effective utilization of the finite computer-resource. Mesh structures should not be excessively expensive to employ or exhaust the finite computing-resource and yet ensure that the user has confidence in the predictions. In summary, too coarse a grid leads to flow details not being captured (i.e. missed) and the conclusions from the numerical procedure not adequately representing the physics contained in the full partial

differential equations (PDEs) of the continuity, momentum, energy and species equations. Too fine, and the computing cost becomes too high.

Before attempting to solve the problems, it is needed to validate that the obtained results don't change with the level of unacceptable percentages when the quality and density of the mesh is changed. In other words, it is needed to validate the results are not highly mesh dependent. A mesh dependent model is

The validation is done with a single 3D model. 4 different type of mesh quality is used. The number of elements for each mesh quality is assigned as they are linearly increased as possible. The outlet temperature values for each element numbers are given in Table 2.6.

Table 2.6: Change in the outlet temperatures with respect to change in number of elements in a single model

Number of elements	**Outlet Temperature**
1507284	306,32
750957	306,28
378061	306,29
233565	306,3

According to obtained results, the model is not highly mesh dependent and highest error is calculated as %0.006.

3 VALIDATION RESULTS

6 different 3D models and porous models were calculated separately. 3D models and porous models are compared in terms of temperature gradients across the fluid directions and pressure drops.

The temperature data are taken from same locations from both types of models, porous and 3D. Therefore, in each type of model, data probes are located right in the middle of the channels and porous domain. The image shows the location of the line probe is shown in Figure 3.1.

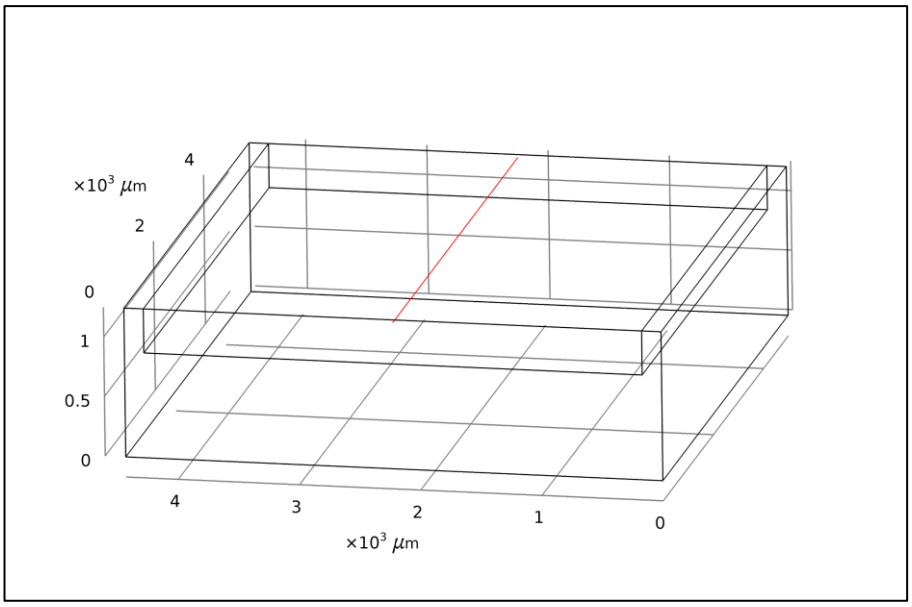

Figure 3.1: Data line probe for acquiring temperature data from the location of the line

3.1 Comparisons of Temperature Changes Across a Single Channel

After placing data probes to each type of models, computational analysis is made using COMSOL software. All data probes give data to create a temperature plot for the corresponding models. These temperature plots were compared with their respective matches. The temperature plots for each channel sizes are shown in Figure 3.2 to 3.4.

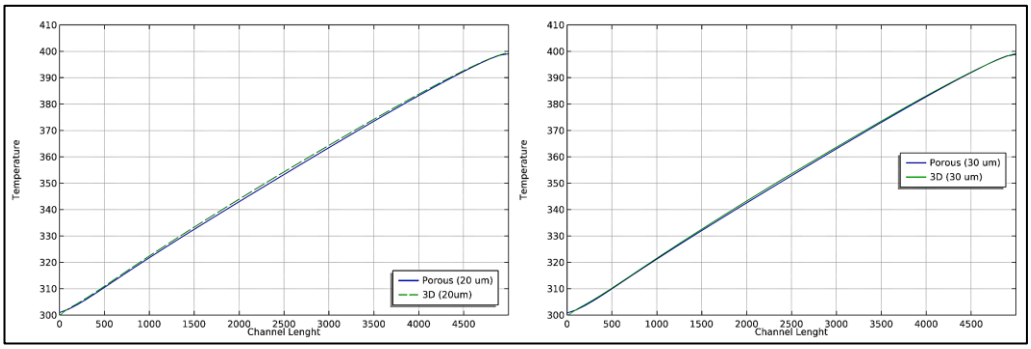

Figure 3.2: from left to right 20 and 30 um 3D and porous model temperature curves taken from data line in Figure 6

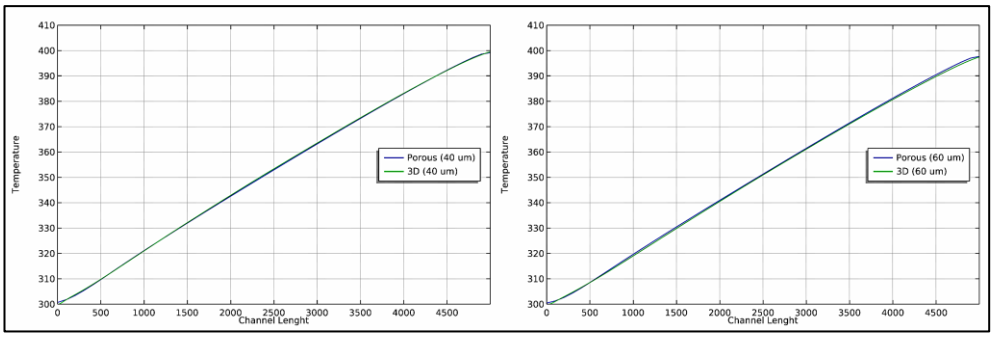

Figure 3.3: from left to right 40 and 60 um 3D and porous model temperature curves taken from data line in Figure 6

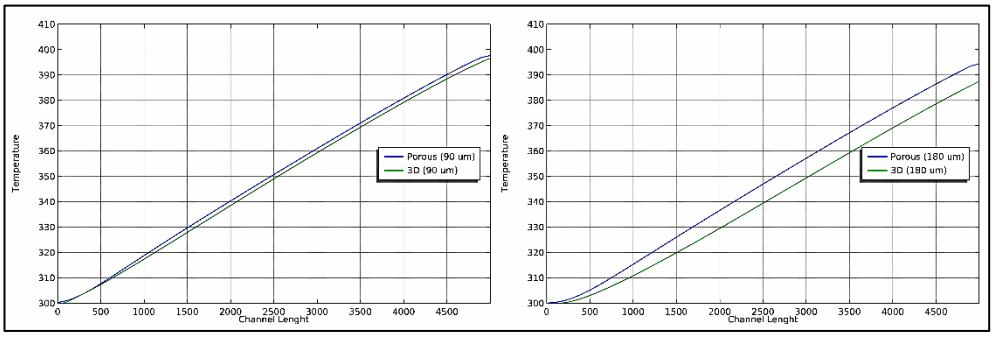

Figure 3.4: from left to right 90 and 180 um 3D and porous model temperature curves taken from data line in Figure 6

As seen from the tables, temperature graphs for six different models are created using the data that is taken from data probes that are placed to 3D and porous approximated models. Temperature data from 3D and porous models of each sizes are compared with each other and represented on the plots above. Also, an overall temperature plots for porous and 3D models are shown in Table 3.5 and 3.6 respectively.

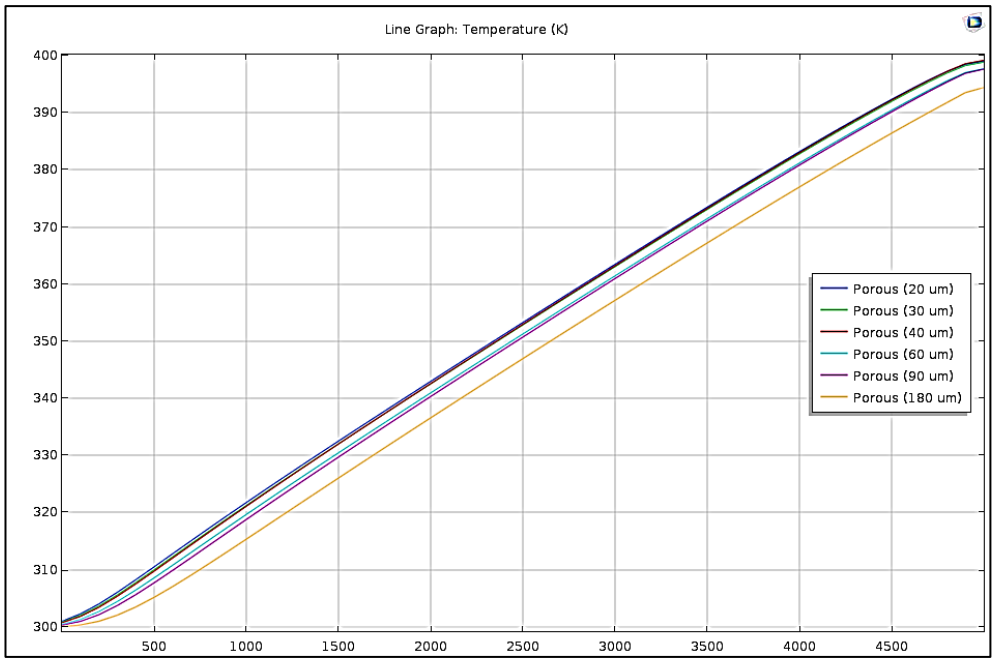

Figure 3.5 :Overall temperature curves for porous models

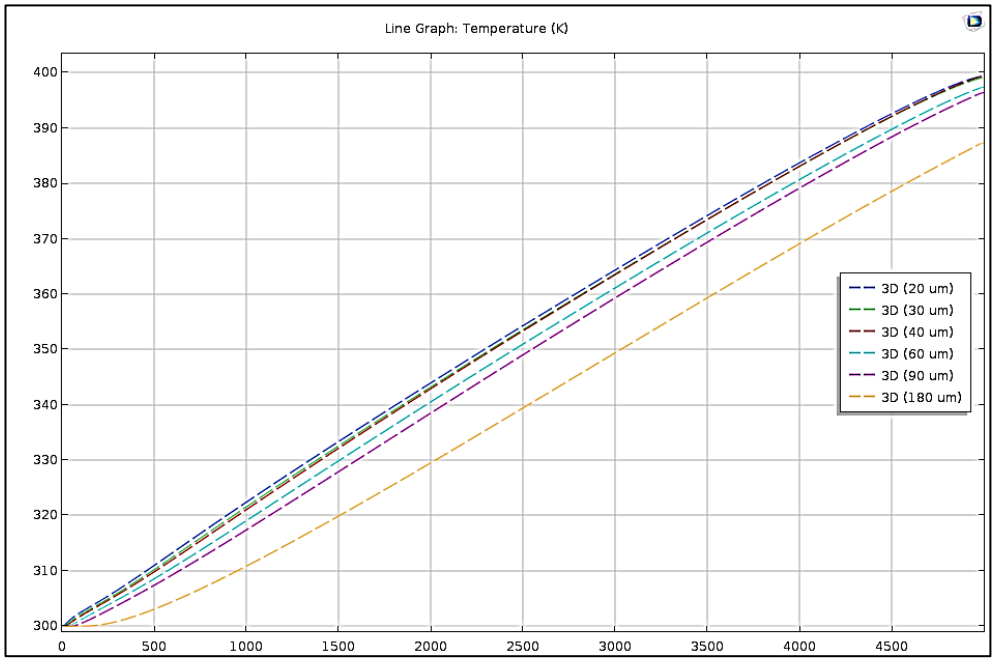

Figure 3.6: Overall temperature curves for 3D models

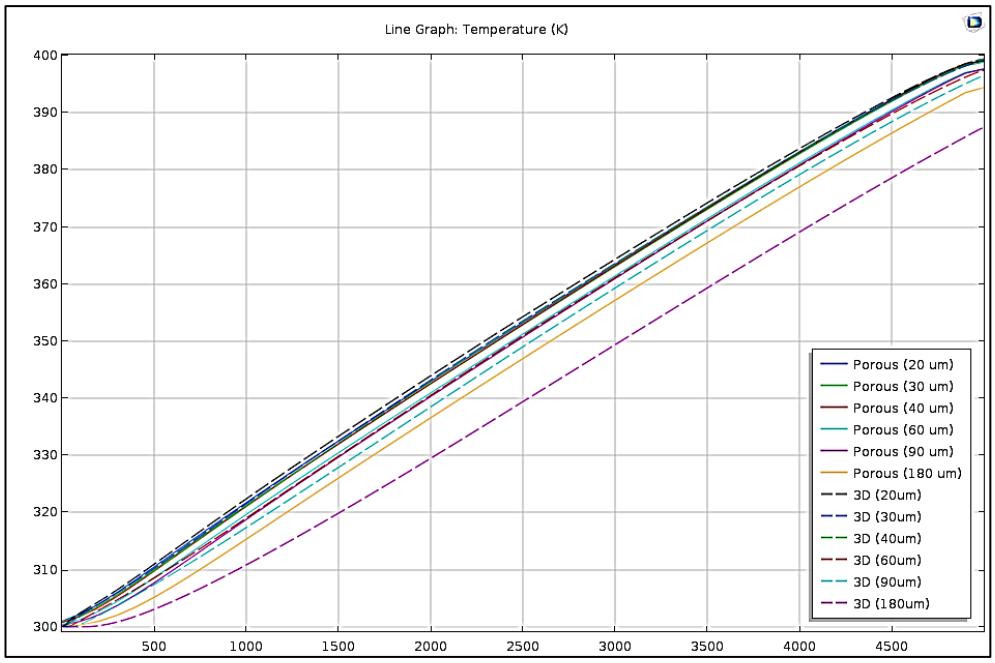

Figure 3.7: Total view of temperature curves of 3D and porous models

An overall temperature gradient comparison graph of 3D and porous models in Figure 12 shows that the porous approximations begin to fail after 90 um channel width since the temperature curves begin to separate. This can be regarded as a limitation of the porous approach.

3.2 Heat Gradients Over Whole Body

The results above is comparisons of the data obtained from a heat probe that is placed along a single channel. To obtain more satisfying results and make a general comparison, it is needed to use more powerful probes that can collect more heat data than a single line probe. Thus, more realistic comparisons can be made. Within this scope, two planar heat probes are placed two different locations on the microchannel. Unlike line heat probes, planar heat probes provide data of a heat gradients of a selected plane. This data when visualized presents more broad heat distribution results.

The results obtained from these two different planar heat probes are visualized as heat contours. Heat contours are indicator of identical heat distributions across a surface. Namely, the similar heat levels are shown as colored ribbons. If there is a different level of heat then the color of the ribbon changes. Heat contours provides a

more abroad view of how heat is distributed and enable us to see the heat gradient differences between 3D and porous models.

Probes are placed two different locations. One of them is placed right to the symmetry plane and other is placed so as to cut microchannel heat exchanger vertically in two. The images that shows the locations of the data planes which is located to symmetry plane and cut plane respectively are shown in Figure 3.8. During the post process, heat data are visualized by using the data obtained from these planes.

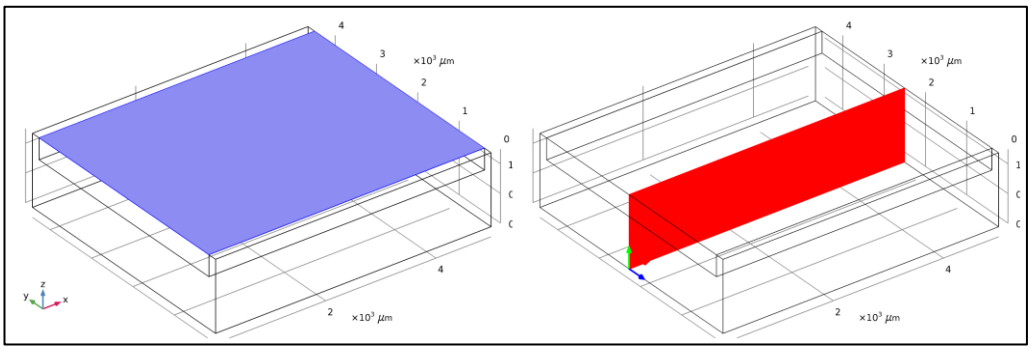

Figure 3.8: Symmetry and vertical data planes which supply temperature data for heat gradients on symmetry plane

3.3 Symmetry Plane Heat Gradients

One of the planes described before was the one that is placed right to the symmetry plane. The symmetry plane is the location that cut the microchannel in half and is an important location since the fluid flow is flowing through here. With the data obtained from here, effect of no slip conditions on channels, heat gradient of fluid flow on porous and 3D models can be examined.

On Figure 3.9, heat gradient contours on the symmetry plane of the 20um microchannel is shown. 3D model and porous model is shown on the figures from left to right respectively. The patterns of contours are greatly similar. But the maximum heat level on porous model differ from 3D model by %0.5.

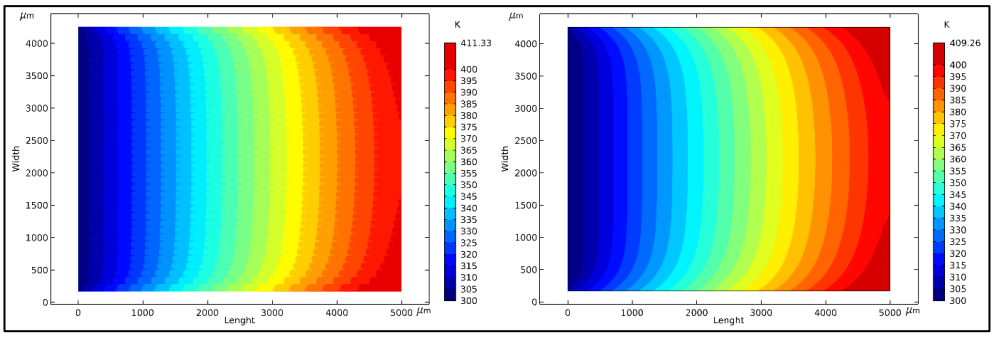

Figure 3.9: 20 um micro channel heat gradient of 3D and porous models on symmetry plane

On Figure 3.10, heat gradient contours on the symmetry plane of the 30um microchannel is shown. The patterns of contours are greatly similar. But the maximum heat level on porous model differ from 3D model by %0.6.

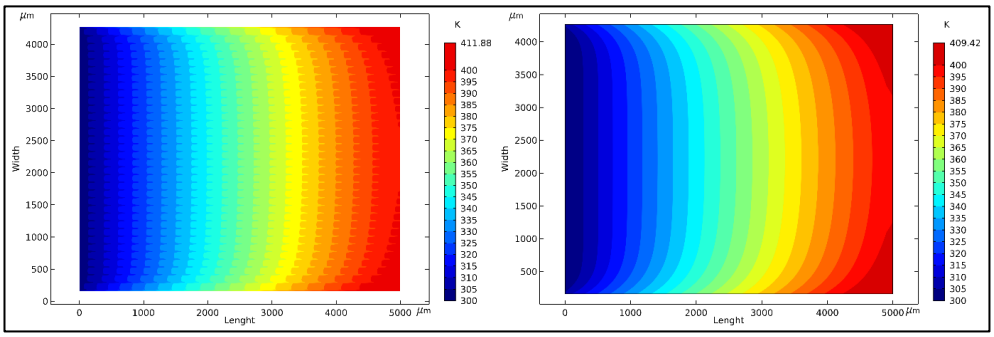

Figure 3.10: 30 um micro channel heat gradient of 3D and porous models on symmetry plane

On Figure 3.11, heat gradient contours on the symmetry plane of the 40um microchannel is shown. The patterns of contours are greatly similar. But the maximum heat level on porous model differ from 3D model by %0.36. From this point on, the effect of no slip condition on heat gradients can be seen distinctively.

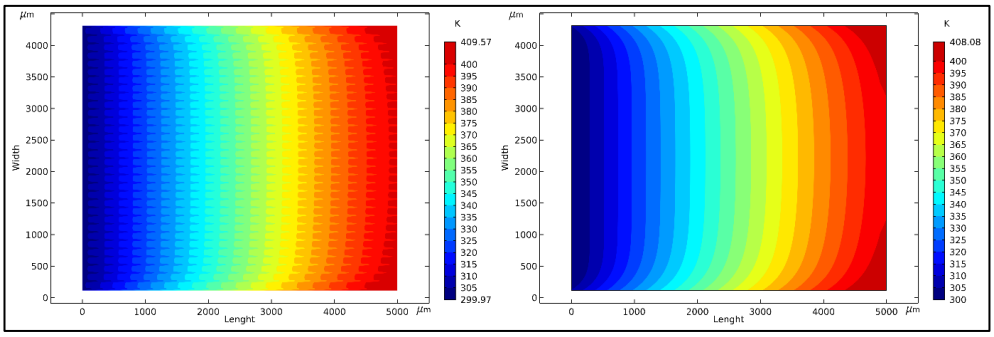

Figure 3.11: 40 um micro channel heat gradient of 3D and porous models on symmetry plane

On Figure 3.12, heat gradient contours on the symmetry plane of the 60um microchannel is shown. The patterns of contours are greatly similar. But the maximum heat level on porous model differ from 3D model by %0.97. Again, the effect of no slip conditions decreased since the channel width is increases. Namely, No-slip condition can no longer hold the flow and let the flow at the center of the channels go faster than from the walls and make a distinct parabolic flow pattern.

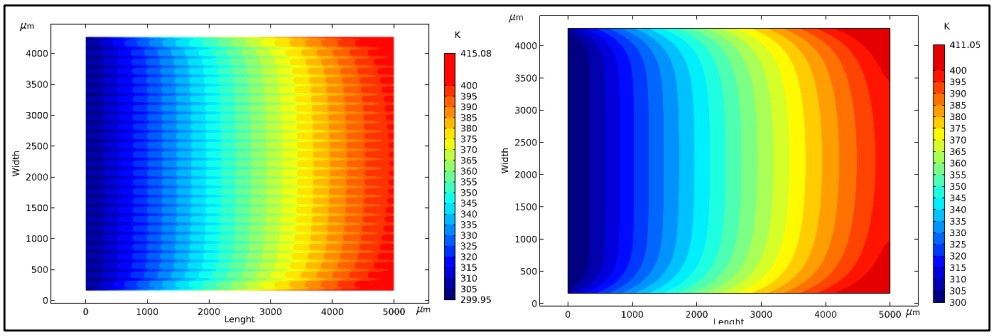

Figure 3.12: 60 um micro channel heat gradient of 3D and porous models on symmetry plane

On Figure 3.13, heat gradient contours on the symmetry plane of the 90um microchannel is shown. The patterns of contours are greatly similar. But the maximum heat level on porous model differ from 3D model by %0.79.

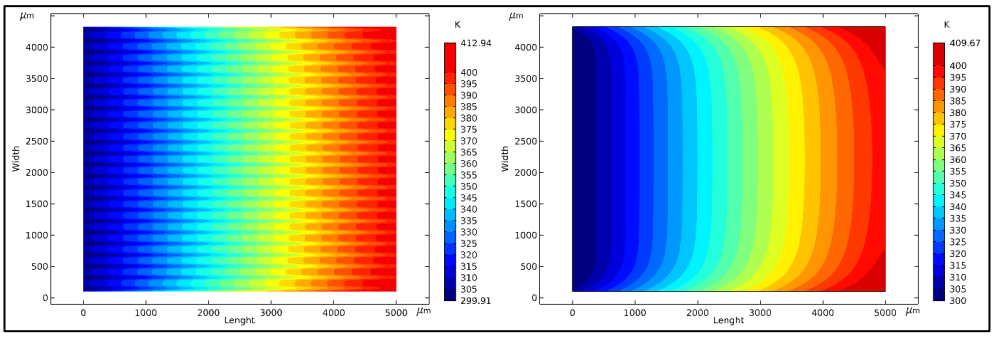

Figure 3.13: 90 um micro channel heat gradient of 3D and porous models on symmetry plane

On Figure 3.14, heat gradient contours on the symmetry plane of the 180um microchannel is shown. The patterns of contours are greatly similar. But the maximum heat level on porous model differ from 3D model by %2.4. Effect of increase in channel width increased on 180um model.

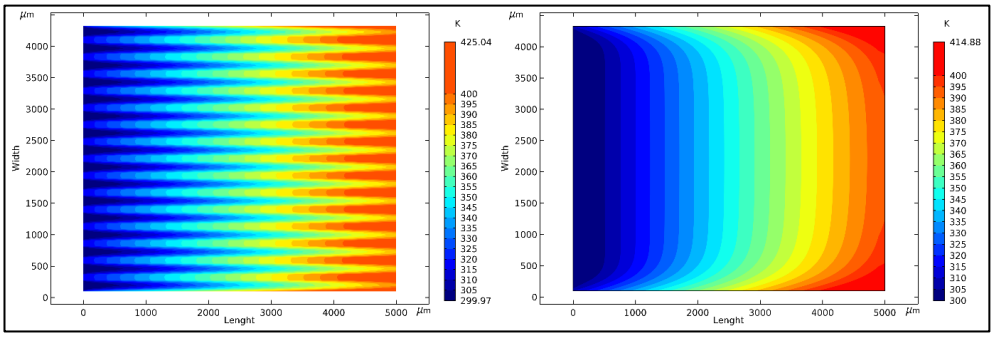

Figure 3.14: 180 um micro channel heat gradient of 3D and porous models on symmetry plane

3.4 Vertical plane heat gradients

As explained before a vertical plane is put in the middle of the whole model cutting the model vertically in half. From data taken from this plane, the temperature gradient on solid and fluid domain can be seen. 3D model and porous model is shown on the figures from left to right respectively.

On the models with 20um channel width as seen from the Figure 3.9, the heat gradient contours show great similarities. The maximum and minimum heat levels are nearly same. But in 3D model as seen in the Figure 3.15 on the left side, as in symmetry

plane, effects of no-slip condition show itself as a small diffraction on the line that represents bottom surface of single channel.

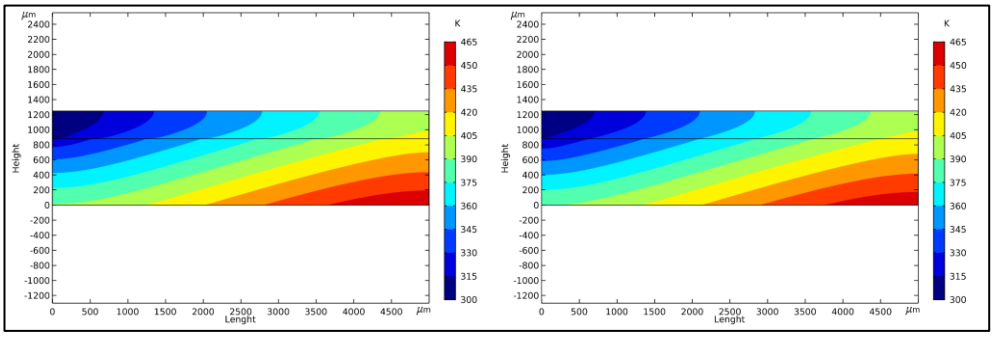

Figure 3.15:20 um micro channel heat gradient of 3D and porous models on vertical plane

On the models with 30um channel width as seen from the Figure 3.16, the heat gradient contours show great similarities. The maximum heat levels are nearly same.

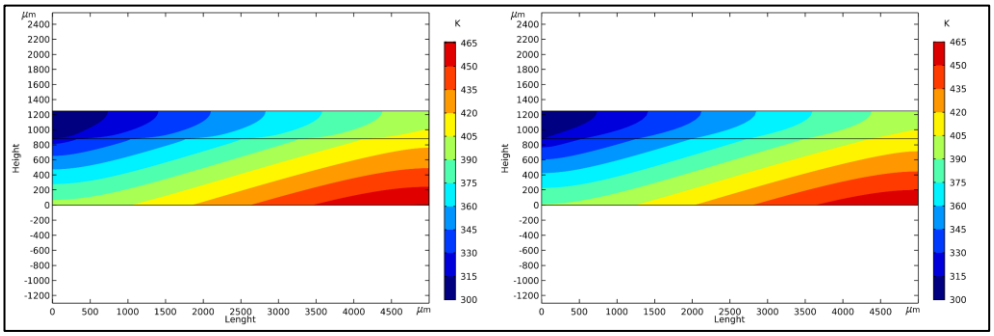

Figure 3.16: 30 um micro channel heat gradient of 3D and porous models on vertical plane

On the models with 40um channel width as seen from the Figure 3.17, the heat gradient contours show great similarities. The maximum heat levels are nearly same.

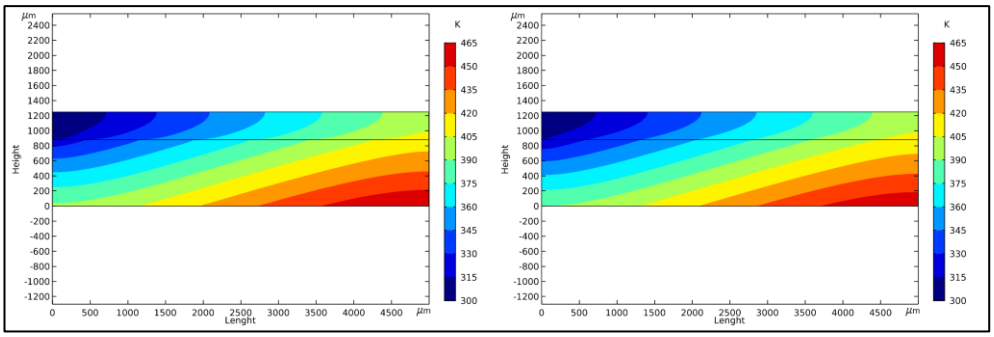

Figure 3.17: 40 um micro channel heat gradient of 3D and porous models on vertical plane

On the models with 60um channel width as seen from the Figure 3.18, the heat gradient contours show great similarities. The maximum heat levels are nearly same.

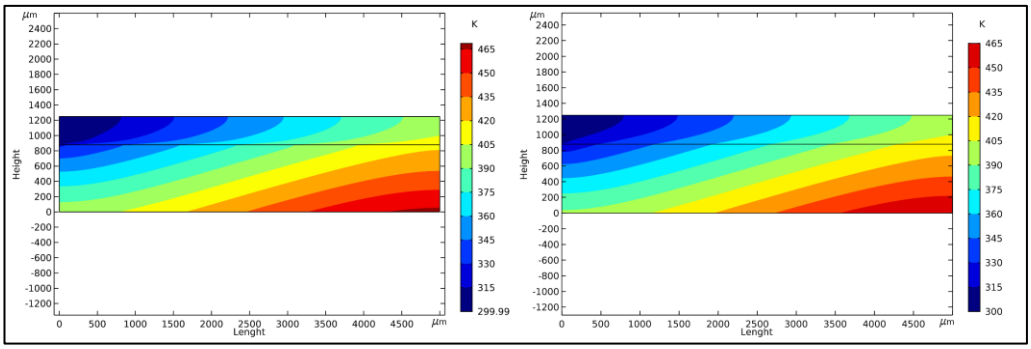

Figure 3.18:60 um micro channel heat gradient of 3D and porous models on vertical plane

On the models with 90um channel width as seen from the Figure 3.19, the heat gradient contours of the porous model slightly differ from the 3D model. This is the beginning of the limit of porous medium approach. Maximum heat level across the porous model is %2 lower than 3D model.

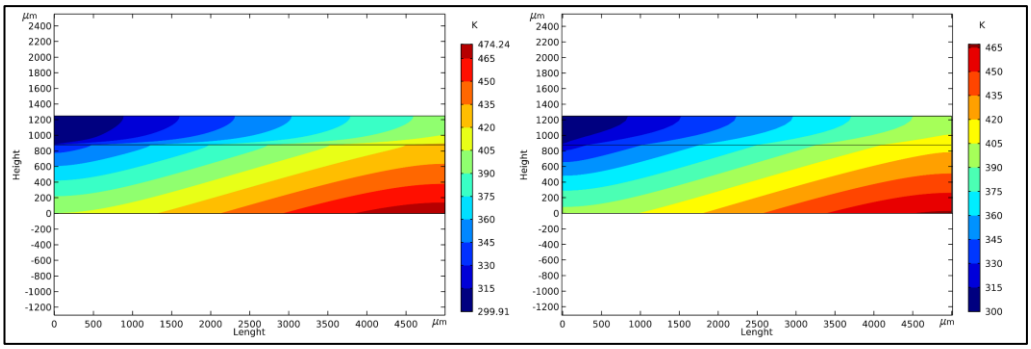

Figure 3.19: 90 um micro channel heat gradient of 3D and porous models on vertical plane

On the models with 180 um channel width as seen from the Figure 3.20, difference in the heat gradient contours between the models is higher that 90 um model.

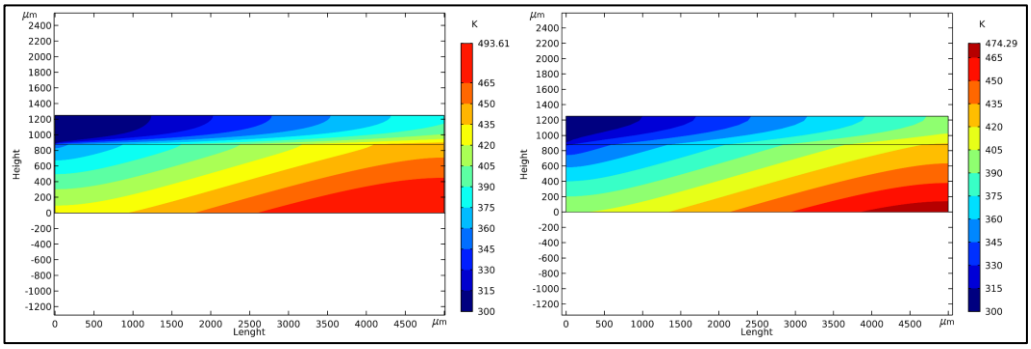

Figure 3.20:180 um micro channel heat gradient of 3D and porous models on vertical plane

3.5 Pressure Drop

Another comparison between 3D and porous approximated models are made in terms of pressure drops across the fluid domains. Pressure drop is an important indicator to measure the how proper the approximation is.

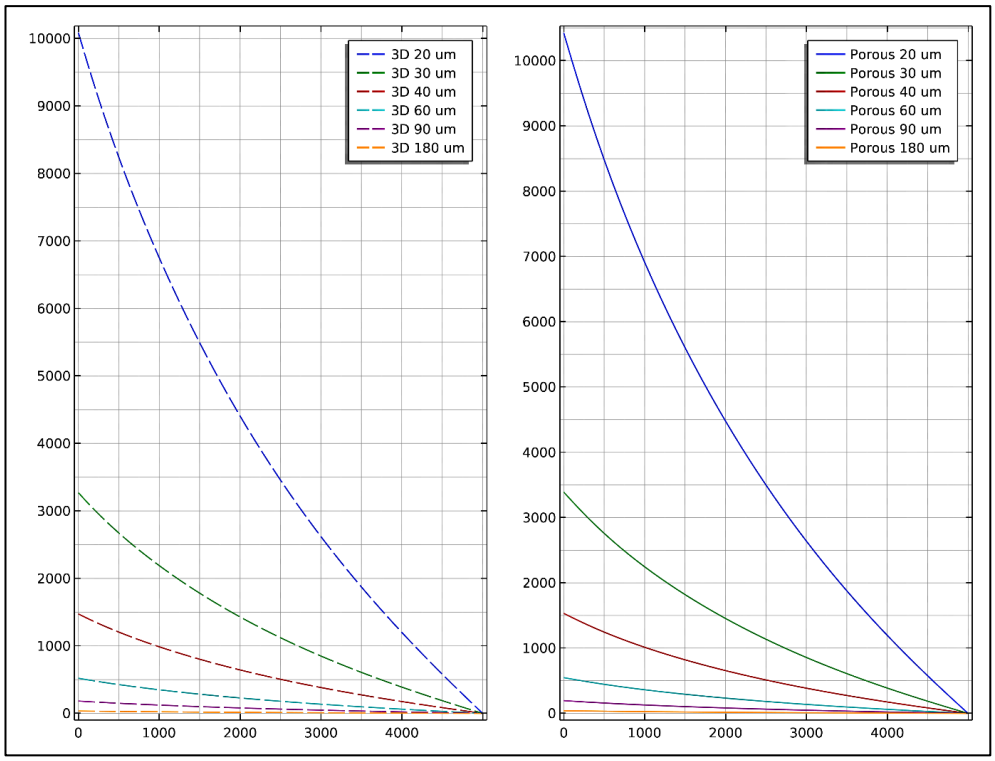

Figure 3.21: Pressure drops across the data line shown in Figure 6

As seen from the Figure 3.21, pressure drop measurement for 3D and porous models show great similarities.

3.6 Computation Time

Reducing calculation time is the most important aim in this study. All channels in a 3D model can be reduced to a single domain using the porous media approach described above. This is the main principle behind the struggle of reducing computation times. Thus, more complex channel geometries can be reduced to a group of porous domains so is computation time.

To see how porous approach spends the least time for the analysis, there presented a comparison chart between porous and 3D model analyses in Table 3.1.

Table 3.1: Computation times of 3D and porous models

Channel Size	3D	Porous
20	2h 55 m	17 m
30	2h 20 m	21 m
40	2h 22 m	17 m
60	1h	19 m
90	1h 21 m	19 m
180	1 h 18 m	33 m

According to the Table 3.2, porous approach spends up to 7 times lesser time than 3D analysis. This provides great flexibility in numerical analysis since most of the time, analyzer realizes if there is a mistake or not after the end of the analysis. This causes analyzer to lose too much time in case of a failure.

Moreover, the porous approach provides lesser computational load to the computer that makes the analysis. The Table 2.5 also shows the total amount of elements used in porous and 3D analyses. The more element means more computational loads. Sometimes when using a regular computer, the computational loads exceed the maximum memory and processing capacity of the hardware. This is often frustrating and limiting researcher from doing simulations.

4 MALDISTRIBUTION

Flow maldistribution is a particular concern in compact heat exchangers as they are typically comprised of many small channels while maldistribution of flow is a primary reason for poor heat transfer performance. The term maldistribution can be described as flow irregularities on channels resulting from channel clogs, manifold related flow irregularities etc. Maldistributions prevents microchannels from dissipating heat that is required to taken away. from the heat source.

In real life problems, flow maldistributions occur generally in complex structure. It is really hard process to simulate and analyze this type of problems. On the other hand, maldistribution scenarios can be created using some mathematical models to simulate real life problems. But these scenarios can never reflect the true mechanism of the maldistribution but can give an approximate result. By using these mathematical

assumptions, heat transfer and fluid flow analyses for maldistribution can be made. Results obtained gives a general idea how the heat transfer performance of a microchannel is being affected. Also, these results shade a light into finding proper designs for manifolds and channel structures.

As stated before, it is a hard task to simulate maldistribution problems but they can be modelled by some mathematical models. Nevertheless, solving these mathematical problems by using 3D models is time consuming and costs high amount of computer loads. Right at this point, porous media approximation method helps greatly. Using this approximation and mathematical models, maldistribution problems can be solved in short computer times.

In this scope, maldistribution analyses are made using some mathematical models on the geometrical models that was used in validation processes before. Below, results obtained from the analyses are presented.

4.1 Mathematical Models

5 different maldistribution scenarios are identified. 3 of these flow maldistribution scenarios is manifold related, other two is assumed to happen by environmental conditions. The boundary conditions of these scenarios were kept same with the previous 60um porous medium analysis. Accordingly, the water is flowing through the channels and it is used to cool a heat load of 1 W/mm^2. The descriptions of the scenarios are listed below;

Scenario 1: The manifold that distributes fluid has a linearly narrowing structure. Flow direction can be seen in Figure 4.1.

Scenario 2 :The manifold that distributes the fluid has a parabolic narrowing structure. Flow direction can be seen in Figure 4.3.

Scenario 3: The flow is sent to the channels directly and the velocity curve is assumed to draw a parabola that its center is aligned to the center of channel domain. Flow direction can be seen in Figure 4.5.

Scenario 4: Center of the channels are clogged and flow is flowing through the channels near the walls. It is assumed there is no manifold related interactions here.

Scenario 5: Channels are clogged randomly. It is assumed, as in Scenario 4, there is no manifold related interactions here.

These 5 cases are modelled not by 3D geometries but by mathematical models of inlet velocity profiles to provide simplicity. The mathematical models of the inlet velocity profiles are constructed assumingly. The mathematical models of all these scenarios are created so as they all have same mean. The mean of the equations is calculated using the equation 4.13.

$$\bar{f}(x) = \frac{1}{b-a}\int_a^b f(x)dx \tag{4.13}$$

All these mathematical models are actually velocity equations and to make a proper comparison between the nominal condition and maldistributed, the mean of each equations must be kept same.

The equation form of each model is listed below.

Scenario 1

f1=3*(y)/(2*10^5)+0.0011049

Scenario 2

f2=(y^2)/(2*10^8)+0.0014

Scenario 3

f3=-((y-2215)^2)/10^8+0.04719

Scenario 4

f4=(3*((4*y-2*4430)^2)/10^8+0.01)/20.952

Scenario 5

f5=abs(sin(y/25))/19.7266

4.2 Manifold Related Flow Maldistribution Scenarios

4.2.1 Scenario 1

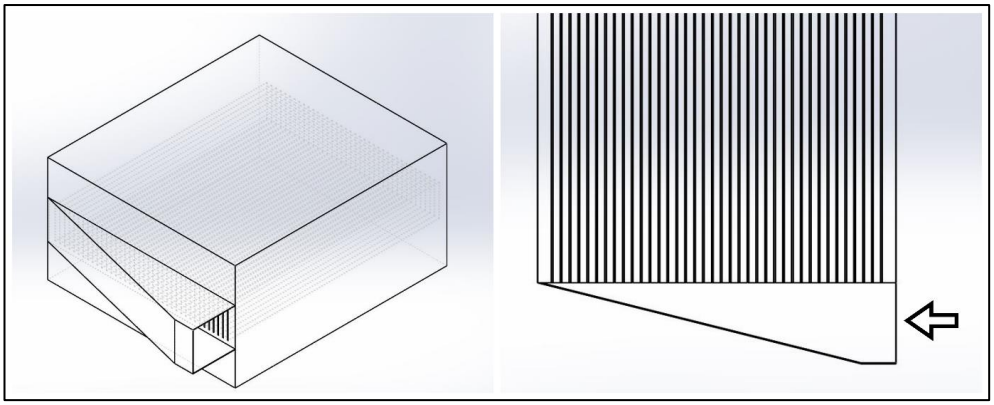

Figure 4.1: Scenario 1 header model and flow direction

In scenario 1, it is assumed that the manifold that distributes the flow has a linearly narrowing structure as seen on the Figure 4.1. Therefore, the velocity profile at the input side of the microchannel model is modelled mathematically as linearly changing as shown on the Figure 4.2. The average fluid flow is kept same with previous

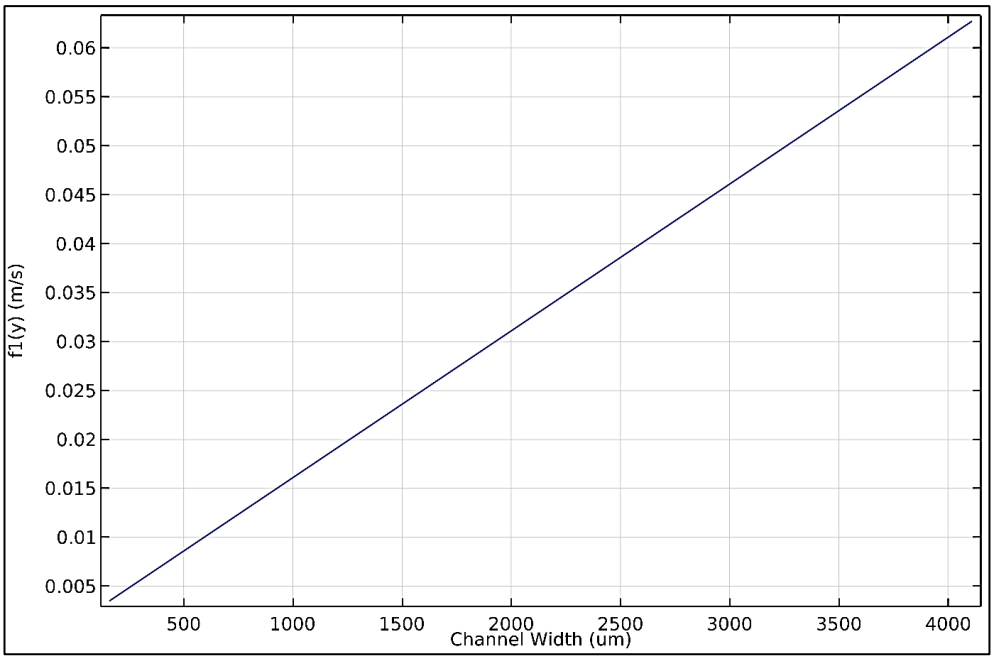

Figure 4.2: Velocity curve at the inlet for scenario 1

4.2.2 Scenario 2

In this scenario, unlike scenario 1, manifold structure at the inlet is not changing linearly but changing by a curve as in Figure 4.3 and it is assumed that the velocity distribution profile at the inlet is parabolic.

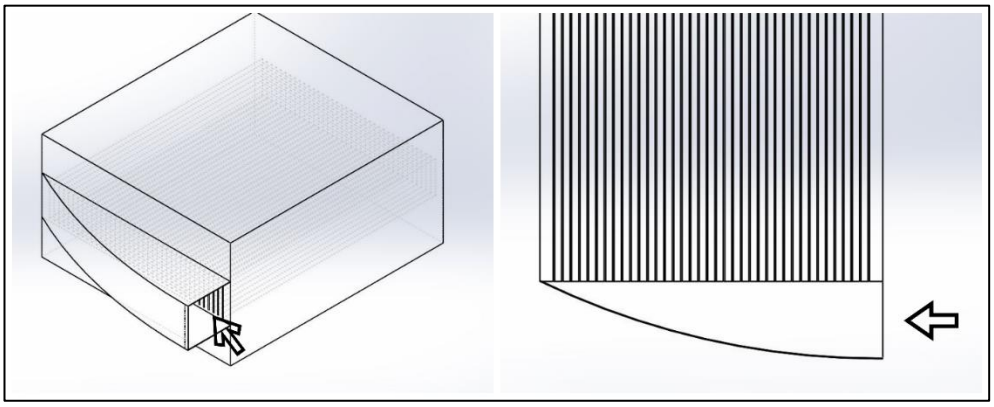

Figure 4.3: Scenario 2 header model and flow direction

According to this assumption, the graph of the mathematical model is shown in the Figure 4.4.

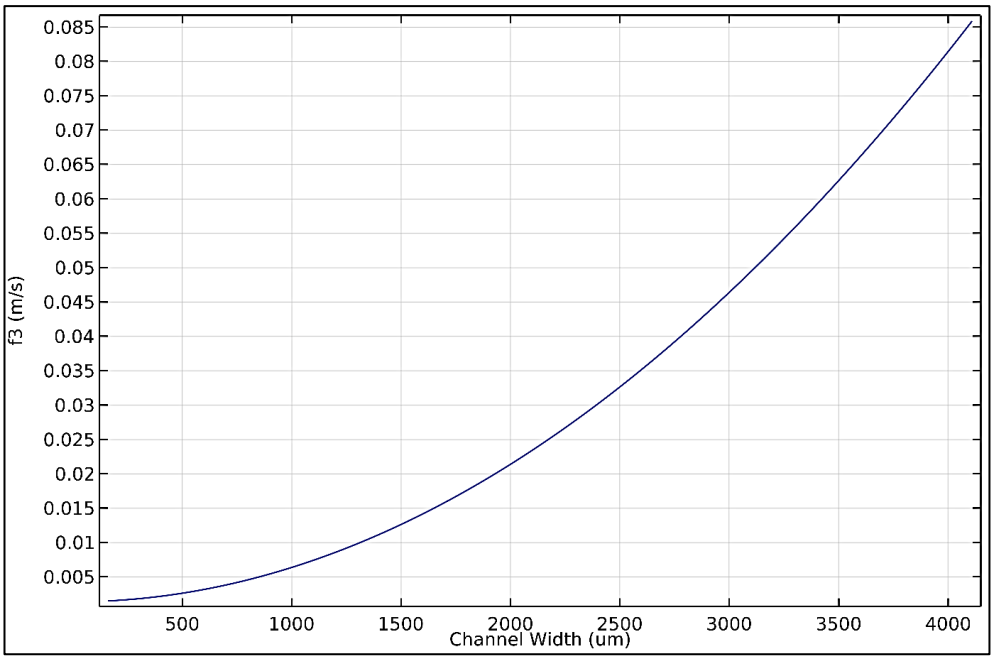

Figure 4.4: Velocity curve at the inlet for scenario 2

4.2.3 Scenario 3

In this scenario, fluid distribution is assumed to be provided by a manifold that sends the fluid in the direction of the channels. the assumed manifold design and the direction of the fluid is shown in Figure 4.5.

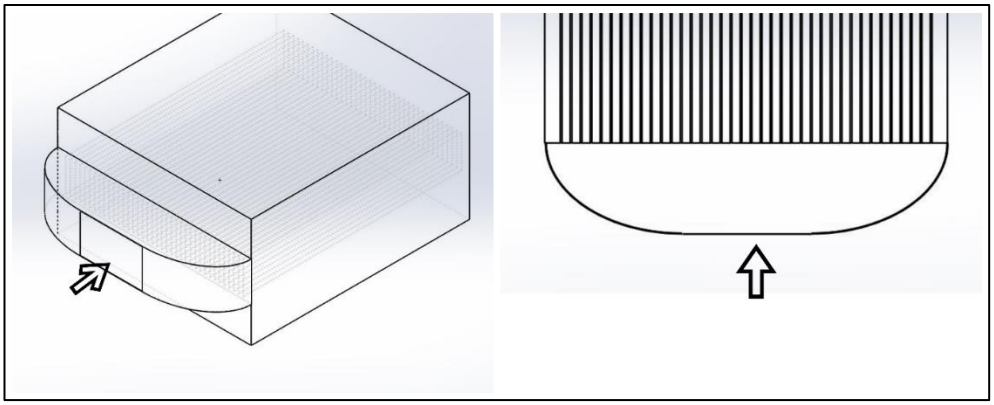

Figure 4.5: Scenario 3 header model and flow direction

This scenario tells that the flow is distributed parabolically across the entrance and the fluid velocity drops near the outer channels. the graphical interpretation of the mathematical model of the velocity profile is shown in Figure 4.6.

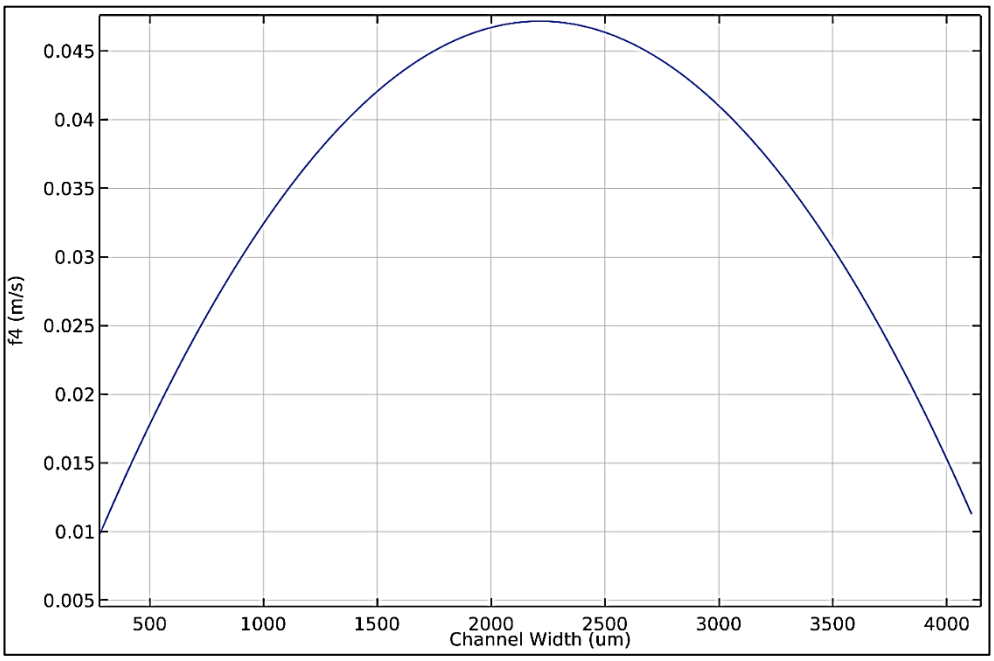

Figure 4.6: Velocity curve at the inlet for scenario 3

4.3 Flow Medium Related Maldistribution Scenarios

Sometimes maldistributions can emerge from the environmental factors such as dirt and foreign particles coming from fluid. Because of the narrow structure of microchannels, these factors can be quite important to consider. A researcher wants likely to know how a microchannel get affected by these unwanted events. Under this header, maldistributions assumed to be occurred by clogged channels.

4.3.1 Scenario 4

In this scenario, Channels located in the middle of the channel group are blocked by dirt and fluid flow can't be provided. Some of the channels near the clogged channels have a slow fluid flow. In this scenario, it is assumed that fluid is sent to channels as evenly distributed and maldistribution is occurred because of dirt.

Graphical interpretation of the mathematical model of this assumption is shown in Figure 4.7 below.

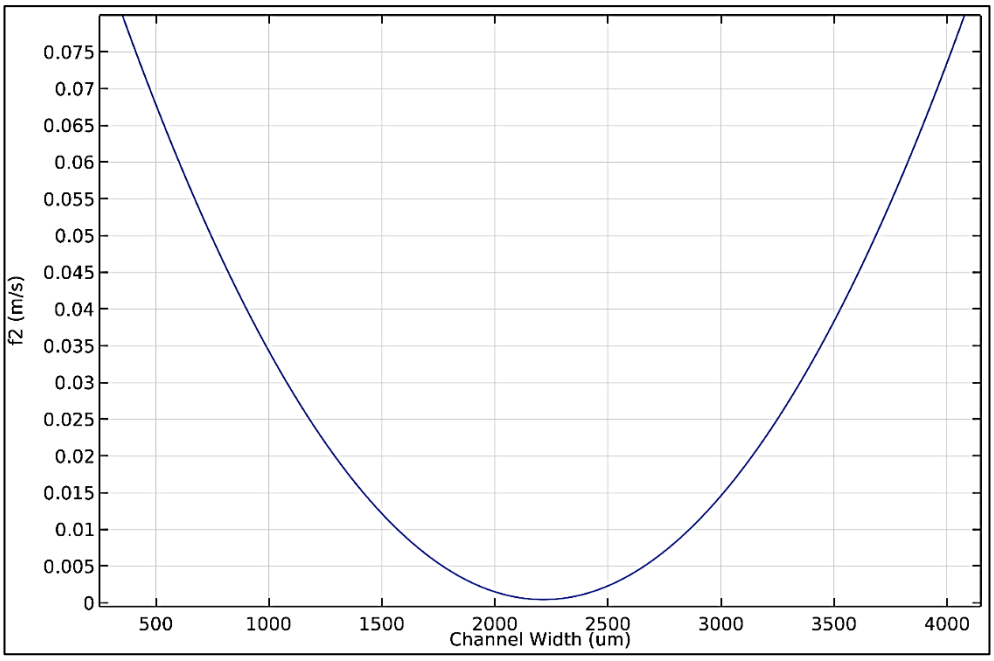

Figure 4.7: Velocity curve at the inlet for scenario 4

As seen from the figure, the central part of the channels has a slow inlet velocity because of channel blockage. Outer side of the whole channel structure is open.

4.3.2 Scenario 5

In this scenario, channels are blocked partially by foreign particles from the fluid flow. Aim is to see how dirt and other foreign particles effect the heat transfer in microchannels. Graphical view of the mathematical model is created using absolute Sin waves. and shown in Figure 4.8.

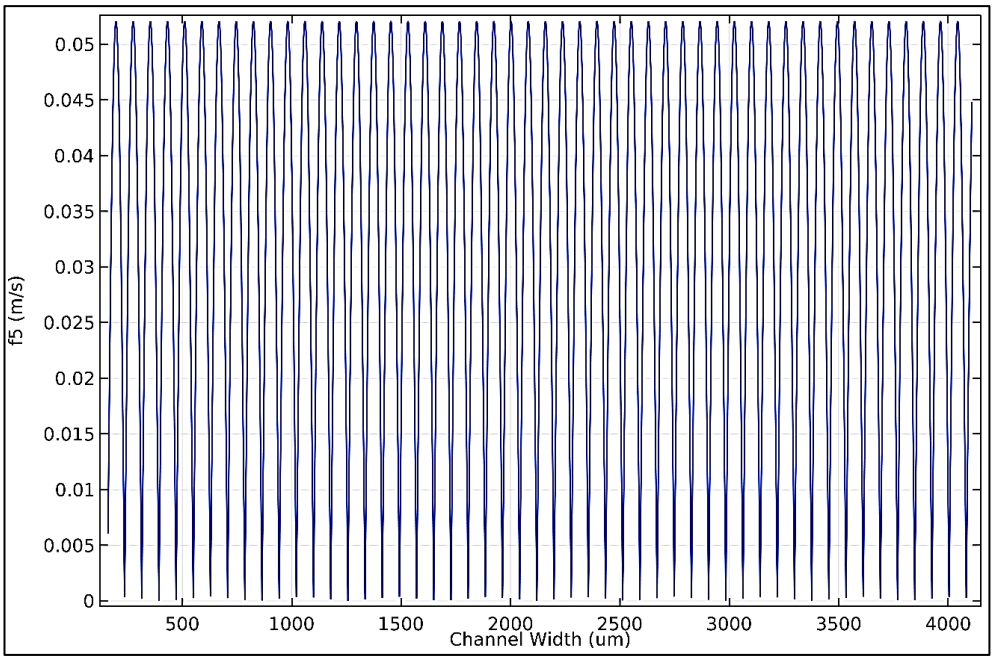

Figure 4.8: Velocity curve at the inlet for scenario 5

All these scenarios are created intending to simulate assumed events on microchannels. Also, it is intented to use previously validated porous media approximation in solving a real-life problem. By doing this, it is also intented to shown how fast the solution to these problems are obtained.

4.4 Analysis Results

CFD analyses of a 60um microchannel is conducted. Porous media approximated model is used. Boundary conditions are kept same with the previous validation analyses. Below, heat gradients and velocity gradients across the symmetry plane is showed. Also, thermal performances are criticized according to maximum heat that is reached on models. For all models, average input velocity is same no matter what mathematical model is used. Thus, for all channels mass flow rate is same.

4.4.1 Scenario 1

According to the results obtained from the analysis, maximum temperature reached in microchannel is 531K. This is %13 higher than the nominal situation. the nominal situation here is all fluid flow entrance velocity is assumed evenly distributed

across the channels. The average outlet temperate increases %4. The thermal effectiveness of the system is decreased.

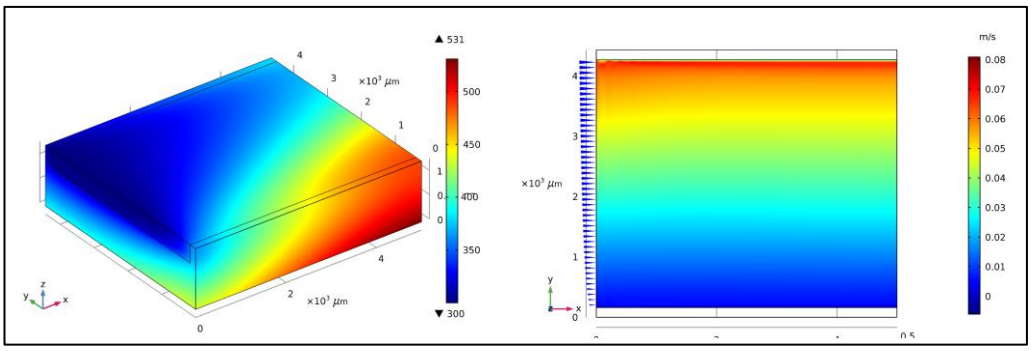

Figure 4.9: Overall temperature gradient of the scenario 1 and velocity distribution across the symmetry plane

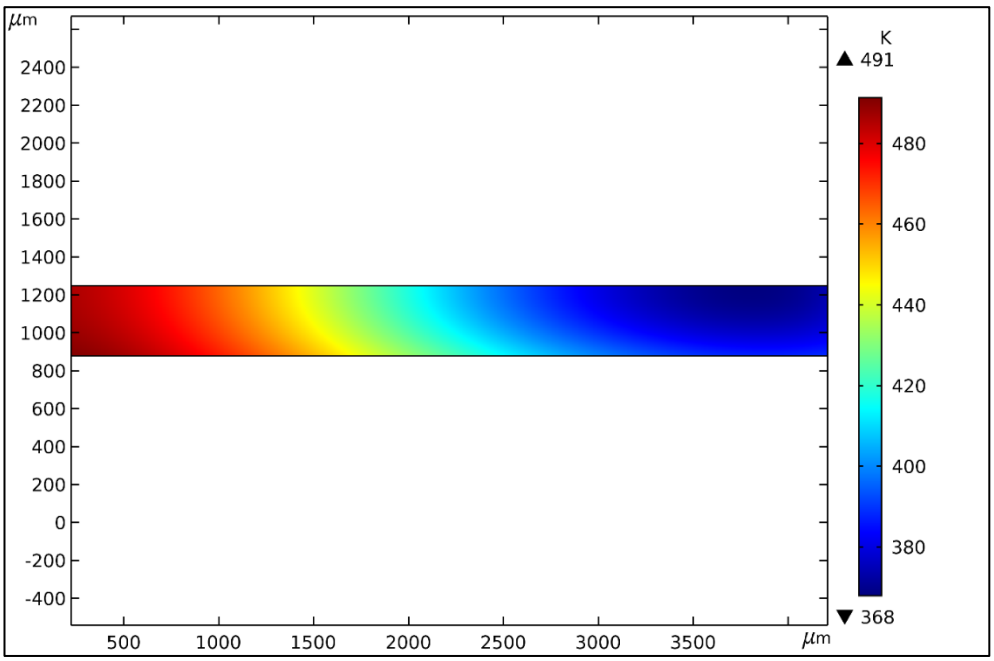

Figure 4.10. Outlet temperature of the model in scenario 1

Table 4.1: Output values of the model in scenario 1

	Scenario 1 Model	Nominal Model
Outlet Temperature (K)	421,5	404,5
Maximum Temperature (K)	531	469
Thermal Effectiveness (K)	0.69	0,7189

4.4.2 Scenario 2

According to the results obtained from the analysis, maximum temperature reached in the microchannel is 557K. This is %19 higher than the nominal situation. General heat gradient of this scenario is similar to scenario 1 but results shows that heat dissipation rates is lower than scenario 1. The average outlet temperature is increased by %6. Termal effectiveness of the microchannel increased. That means this setup is increasing thermal performance of the microchannel.

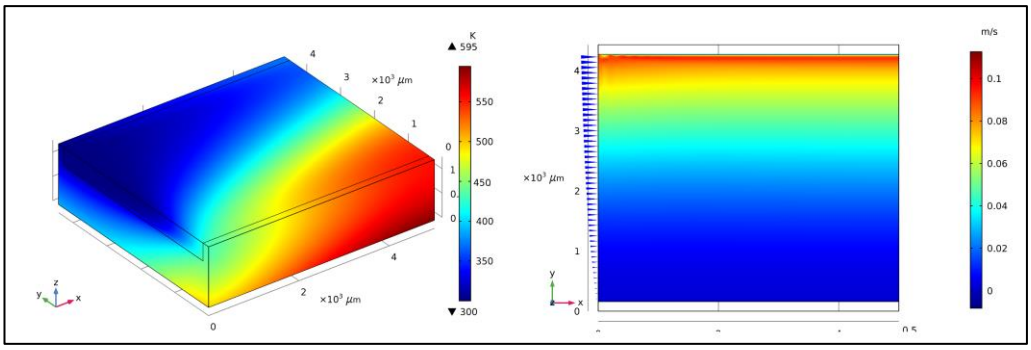

Figure 4.11: Overall temperature gradient of the scenario 2 and velocity distribution across the symmetry plane

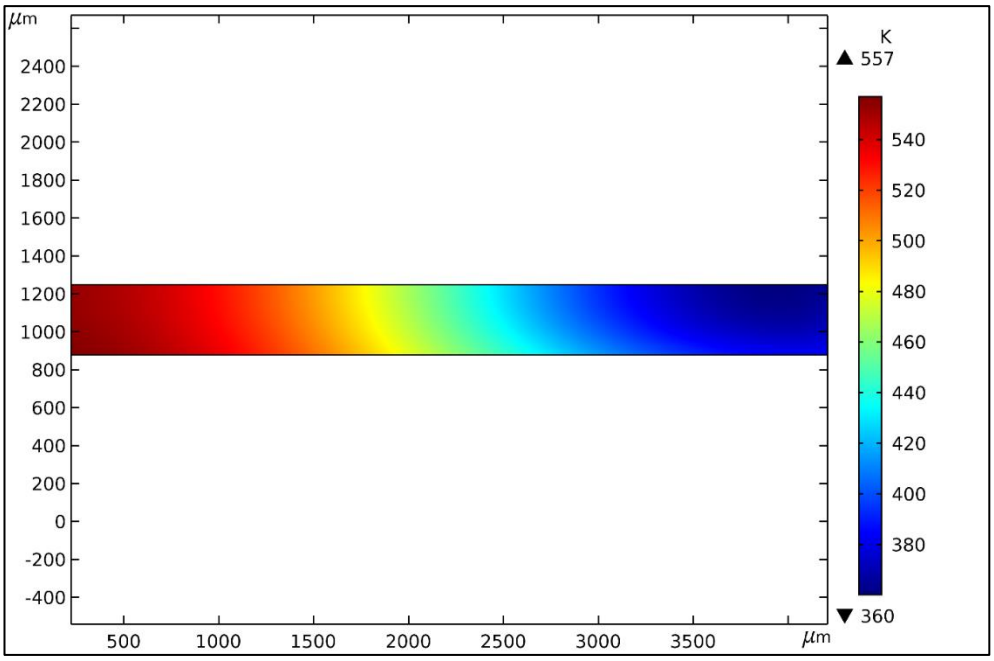

Figure 4.12. Outlet temperature of the model in scenario 2

Table 4.2: Output values of the model in scenario 2

	Scenario 2 Model	**Nominal Model**
Outlet Temperature (K)	426,66	404,5
Maximum Temperature (K)	557	469
Thermal Effectiveness	0,7258	0,7189

4.4.3 Scenario 3

According to the results obtained from the analysis, maximum temperature reached in the microchannel is 484K. This is %3.2 higher than the nominal situation. The average outlet temperature is increased by %2. similar to scenario 2 this setup results performance rise in microchannel system.

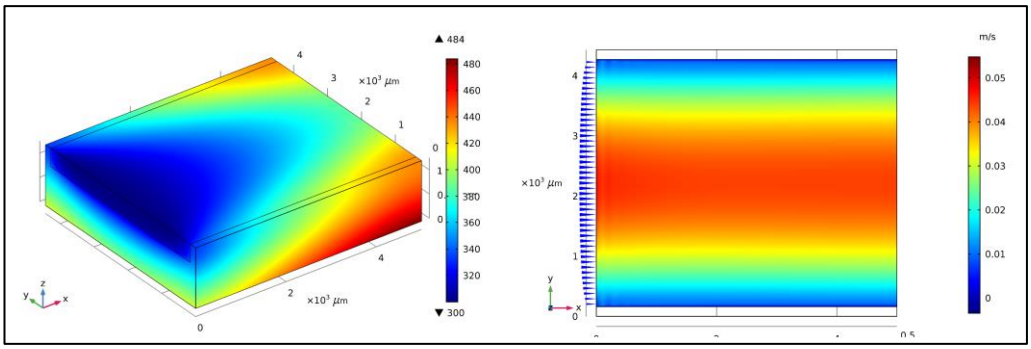

Figure 4.13: Overall temperature gradient of the scenario 3 and velocity distribution across the symmetry plane

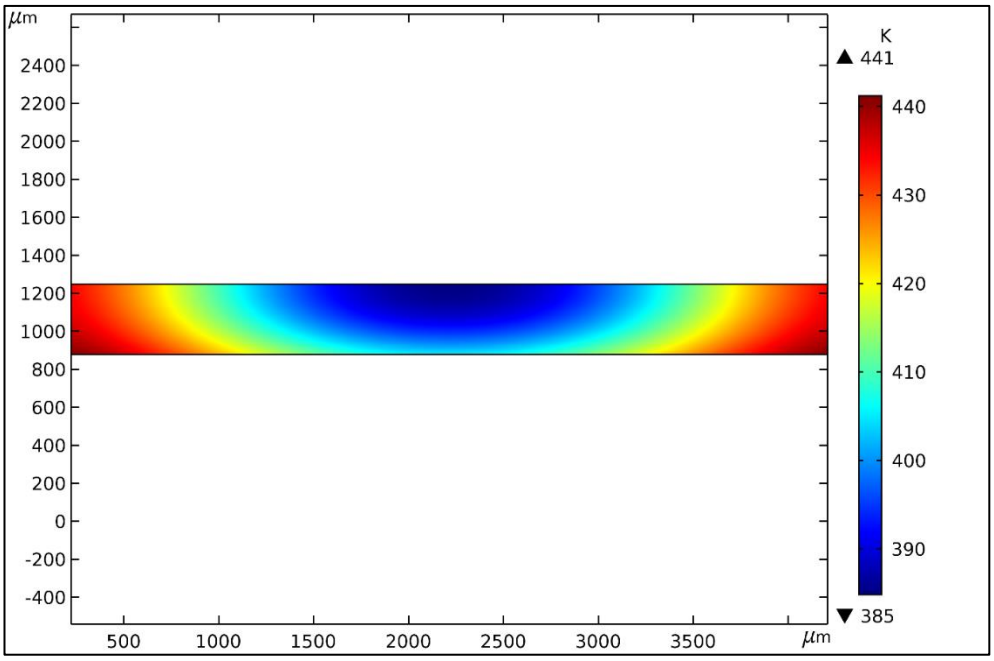

Figure 4.14. Outlet temperature of the model in scenario 3

Table 4.3: Output values of the model in scenario 3

	Scenario 3 Model	**Nominal Model**
Outlet Temperature (K)	411,1	404,5
Maximum Temperature (K)	484	469
Thermal Effectiveness	0,7205	0,7189

4.4.4 Scenario 4

According to the results obtained from the analysis, maximum temperature reached in the microchannel is 501K. This is %6,8 higher than the nominal situation. Average outlet temperature is increased by %2. But unlike the scenario 2 and 3, this maldistribution problem causes a performance loss on the system.

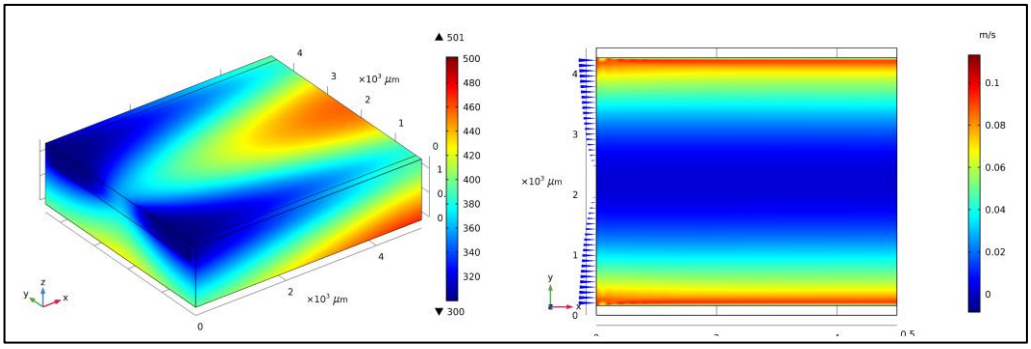

Figure 4.15: Overall temperature gradient of the scenario 4 and velocity distribution across the symmetry plane

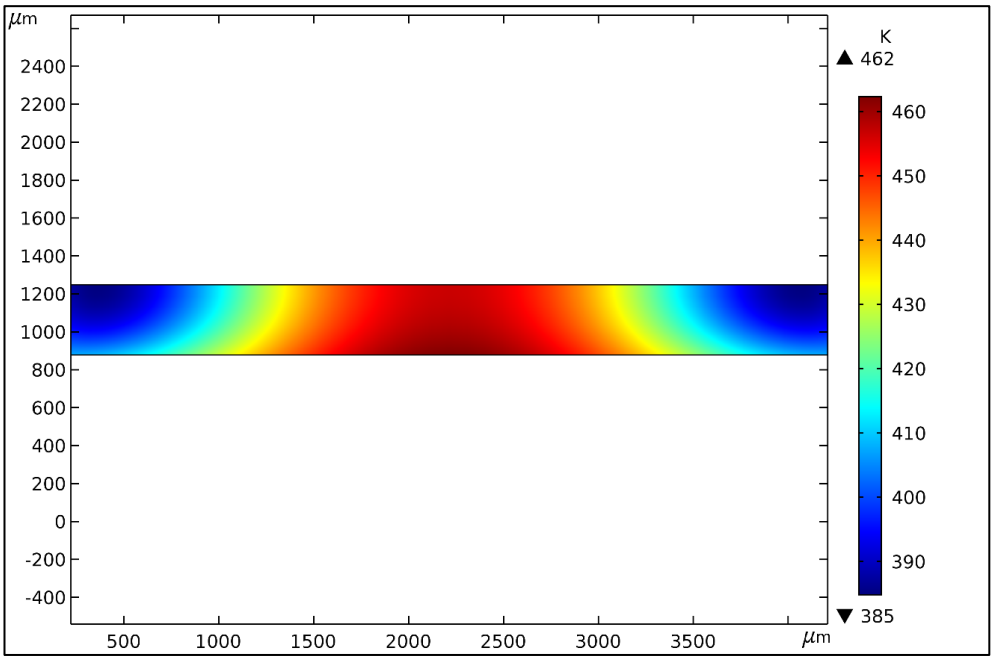

Figure 4.16. Outlet temperature of the model in scenario 4

Table 4.4: Output values of the model in scenario 4

	Scenario 4 Model	Nominal Model
Outlet Temperature (K)	426	404,5
Maximum Temperature (K)	501	469
Thermal Effectiveness	0.7109	0.7189

4.4.5 Scenario 5

According to the results obtained from the analysis, maximum temperature reached in the microchannel is 474K. This is % 1.1 higher than the nominal situation. Average outlet temperature is increased by %0.7. similar to scenario 4, this maldistribution problem causes a performance drop in the system.

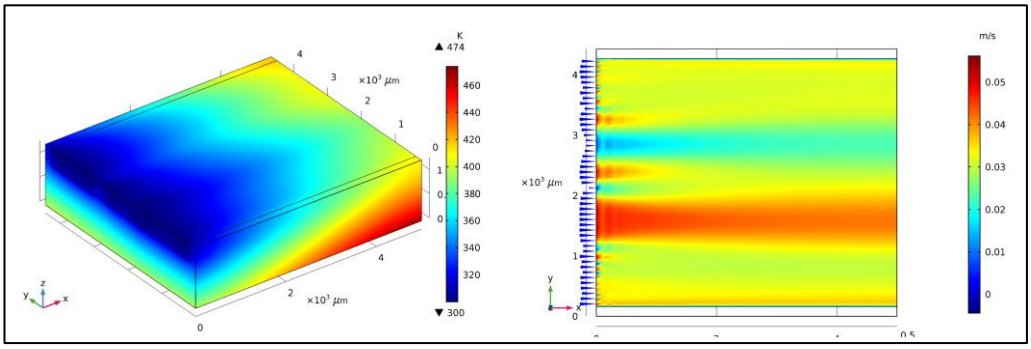

Figure 4.17: Overall temperature gradient of the scenario 5 and velocity distribution across the symmetry plane

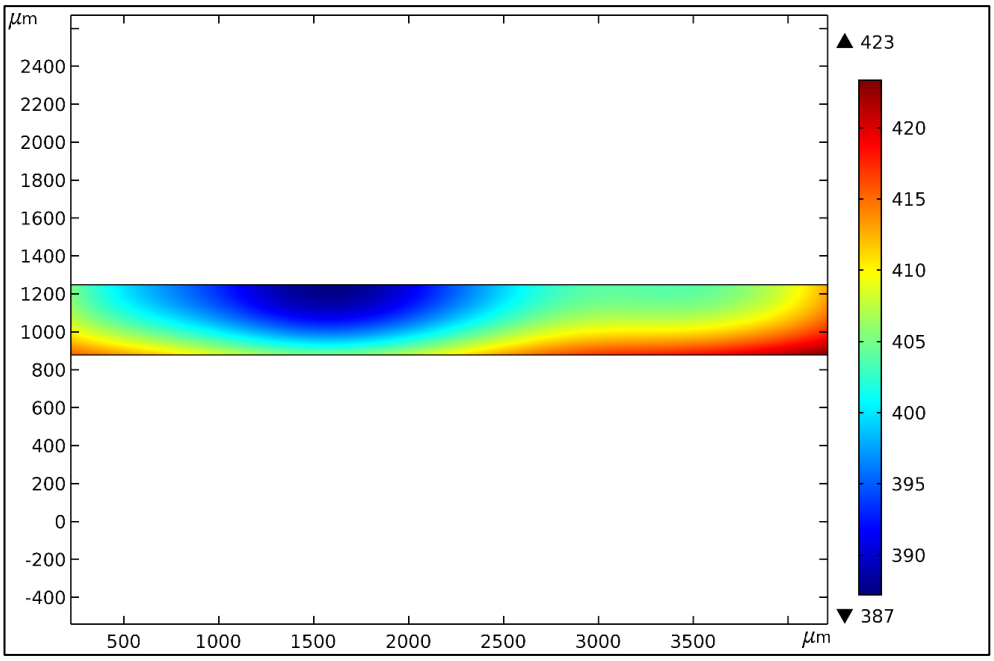

Figure 4.18. Outlet temperature of the model in scenario 5

Table 4.5: Output values of the model in scenario 5

	Scenario 5 Model	**Nominal Model**
Outlet Temperature (K)	407	404,5
Maximum Temperature (K)	474	469
Thermal Effectiveness	0,7155	0,7189

4.5 Discussion About Maldistribution

The flow maldistributions occurred in microchannels has two major cause; the manifold design and environmental flow conditions or a combination of these two. Whatever the cause is, if researcher wants to know what to do about design and other problems, a general over view of the effects of certain designs should be seen by numerical methods visually. These numerical methods sometimes require all models to be modelled as 3D or they are approximated by certain mathematical models. In this study, maldistribution analyses were conducted using some assumptions and mathematical maldistribution models. Of course, there are other parameters that should be taken into account like velocity vectors from other directions except x direction that is used as a flow direction here. In real-life problems, the manifolds used

to distribute fluid into the channels not only distribute it into one direction but also to other two directions naturally. The other components of the flow vectors can change the results obtained here dramatically. Of course, this is a further research topic. To provide simplicity, the flow is assumed to be developed only one direction in the study. Furthermore, an analysis of 3D models of the manifolds will surely give more accurate results. However, struggle to reduce computation time and costs, all manifold designs are represented as mathematical models instead of using 3D models. Each mathematical model created represent an estimated velocity profile. These velocity profiles are thought to be closest approximations to real models. The main parameters that are used when creating these mathematical models are the geometry of the manifold, the direction of the velocity vector and content of other scenarios.

These velocity profiles are assigned as input boundary conditions in all models. This is done by a feature of the software used, the flow velocities can be directly assigned to the boundary as a function.

The results obtained here shows how important factor a manifold design is in the performance of the microchannel heat exchangers since different manifold models shows different velocity and temperature outputs. Researcher can easily acquire a general idea about what change should be made in design or method.

5 GENERAL DISCUSSION

The general intention of this study is to answer some important questions. These are;

-Can 3D modelled microchannel designs be reduced to simpler models to reduce computation time and costs?

-If yes, what are the limitations of the method?

-Within the usability limits of the method, can it be used in maldistribution problems?

-Can velocity profiles at inlet of the models that is used in maldistribution problems be modelled as mathematical models?

-How these manifold models and other scenarios effect the microchannels?

Answering the questions above will also give a general overview of the study.

1st question

When it is asked how to reduce complex problems like flow in microchannels to simpler structures, the first idea that emerges in mind is using the porosity feature of the materials to define structures such as microchannels. At first sight, the microchannel structures and porous medium have something in common. Both structures have a narrow flow passages which can be also called capillary. Another similarity is both channel structure direct flow into a desired direction. In porous media this can be done by using anisotropy feature. As described before, this property can be described by a tensor. By using tensors, a porous medium can be directed to any direction.

The porous medium idea needs more to complete to become a true approximation for 3D structures. It is first needed to be validated with real models. For validation, six microchannel models with six different channels sizes are created. They are analysed with a CFD software. Data taken from different locations on porous and 3D models are compared among corresponding channel sizes. Results from both model type showed great similarities in terms of temperature gradients and pressure drops.

2nd question

The results showed that when the channel size increases, error level also increases. This can be seen apparently in analysis of 90um microchannel. As seen from the temperature gradient graph of 90um porous and 3D models, results from porous medium starts to deviate from the 3D modelled results. This means that results taken from porous models with channels wider than 90um gives improper results. So, it can be said that this approach doesn’t give desired results if model channel is wider that 90um. This can be regarded as the limitation this approach. Of course, this limitation can be pulled to wider channel sizes adding more constraining equations between porous media and 3D geometry.

3rd Question

Within level of acceptable error limits, porous medium approach was used in a row of maldistribution in microchannels analysis. A 60um microchannel is used in different scenarios. Each scenario is based on different type of flow maldistributions. 3 of them is assumed to occur because of manifold design effects 2 of them is assumed to be caused environmental conditions. 60um micro channel is modelled as porous media and given boundary conditions which are used in previous analyses.

4th Question

Rather than modelling each scenario in 3D, they are modelled by mathematical models. Actually, modelled part in computations is velocity profiles. A mathematical model is created assumingly for each scenario and given as boundary condition. After consecutive analyses, results are compared with the nominal results from which porous model with no maldistribution.

In conclusion, most of the time when a researcher study on a computational analysis of microchannels, it is often needed to solve a draft of the model which is full of faults. During solving process, it is sometimes expected to take an error message from the software or sometimes even the error message isn't taken, researcher may not be pleased with obtained results. Most of the time, especially in microchannel analysis, this process takes a lot of time and at the end it can be a frustrating for the one who directs the study. Using tetrahedral meshes solves this problem sometimes but tetra meshed results can be misleading. Using porous media approximation is proved to give up to 7 times faster results and closed to 0 error. This method is also use quad mapped meshes which is more suitable for CFD analyses. Also, it is proven that method can be used in maldistribution analysis in microchannels. Results obtained give a general overview how manifold design and environmental problems effect the heat exchanger efficiency.

5th Question

From the results as seen from the Tables 4.1 to 4.5, different type of manifolds and other maldistribution results result in different effects in microchannel. From the results, the scenario 1, 4, 5 have a performance lost and others are vice versa. The highest performance lost occurred in scenario 1.

REFERENCES

[1] Tuckerman, D. B. (1984). “Heat-Transfer Microstructures for Integrated Circuits”. Ph.D. Thesis, University of California.

[2] Koh, J. C. Y., & Colony, R. (1986). "Heat transfer of microstructure for integrated circuits". International Communications in Heat and Mass Transfer, 13(1), 89–98.

[3] Samalam, V. K. (1989). "Convective heat transfer in microchannels". Journal of Electronic Materials, 18(5), 611–617.

[4] Kim, D.-K., & Kim, S. J. (2006). “Averaging approach for microchannel heat sinks subject to the uniform wall temperature condition”. International Journal of Heat and Mass Transfer, 49(3–4), 695–706.

[5] Kleiner, M. B., Kuehn, S. A., & Haberger, K. (1995)." High performance forced air cooling scheme employing microchannel heat exchangers". IEEE Transactions on Components, Packaging, and Manufacturing Technology. Part A, 18(4), 795–804.

[6] Lasance, C.J.M. & E. Simons, R. (2005). “Advances in High Performance Cooling for Electronics”. 11.

[7] Philips, R.J., 1990. “Micro-Channel Heat Sinks. In: Advances in Thermal Modeling of Electronic Components and Systems”, ASME, Vol. 2, , New York.

[8] Steinke, M. E., & Kandlikar, S. G. (2005). "Single-Phase Liquid Heat Transfer in Microchannels". ASME 3rd International Conference on Microchannels and Minichannels, California,Part B 667–678 (January)

[9] Escher, W., Brunschwiler, T., Michel, B., & Poulikakos, D. (2010), "Experimental Investigation of an Ultrathin Manifold Microchannel Heat Sink for Liquid-Cooled Chips". Journal of Heat Transfer, 132(8), 081402.

[10] Bejan. A. (2004) Convection Heat Transfer, ISBN:9780470900376, Wiley

[11] Sehgal, S. S., Murugesan, K., & Mohapatra, S. K. (2011), “Experimental investigation of the effect of flow arrangements on the performance of a micro-channel heat sink, Experimental Heat Transfer, 24(3), 215–233.

[12] Ming-Chang Lu, & Chi-Chuan Wang. (2006), “Effect of the inlet location on the performance of parallel-channel cold-plate”, IEEE Transactions on

Components and Packaging Technologies, 29(1), 30–38.

[13] Jones, B. J., Lee, P. S., & Garimella, S. V. (2008), “Infrared micro-particle image velocimetry measurements and predictions of flow distribution in a microchannel heat sink”, International Journalof Heat and Mass Transfer, 51(7–8), 1877–1887.

[14] Tonomura, O., Tanaka, S., Noda, M., Kano, M., Hasebe, S., & Hashimoto, I. (2004) "CFD-based optimal design of manifold in plate-fin microdevices", Chemical Engineering Journal, 101(1–3), 397–402.

[15] Morini, G. L. (2004), “Single-phase convective heat transfer in microchannels: A review of experimental results”, International Journal of Thermal Sciences, 43(7), 631–651.

[16] Weisberg, A., Bau, H. H., & Zemel, J. N. (1992),”Analysis of microchannels for integrated cooling”, International Journal of Heat and Mass Transfer, 35(10), 2465–2474.

[17] Arie, M. A., Shooshtari, A. H., Dessiatoun, S. V, & Ohadi, M. M. (2016). “Performance Characterization of an Additively Manufactured Titanium (Ti64) Heat Exchanger for an Air-water Cooling Application”, ASME 2016 Heat Transfer Summer Conference, 1–13, Washington, July.

[18] Kim, S. J., & Hyun, J. M. (2005)," A Porous Medium Approach For The Thermal Analysis Of Heat Transfer Devices In Transport Phenomena In Porous Media", Elsevier, (Pp. 120–146).

[19] Kim, S. J., & Kim, D. (1999),”Forced Convection in Microstructures for Electronic Equipment Cooling”, Journal of Heat Transfer, 121(3), 639.

[20] KAKAC, S. (2013). Heat exchanger selection, rating and thermal design.

[21] Anbumeenakshi, C., Vijaybabu, T. R., & Thansekhar, M. R. (2014),”Experimental Investigation Of Flow Maldistribution In Microchannels”, International Journal of Innovative Research in Science, Engineering and Technology, 3(3), 14–17.

[22] Sobhan, C. B., Sobhan, C. B., & Garimella, S. V. (2001), ”A comparative analysis of studies on heat transfer and fluid flow in microchannels”, Other nanotechnology publications, 5:293-311

[23] Kumaraguruparan, G., Kumaran, R. M., Sornakumar, T., & Sundararajan, T. (2011), “A numerical and experimental investigation of fl ow maldistribution in a micro-channel heat sink”, International Communications in Heat and Mass Transfer, 38(10), 1349–1353.

[24] Vafai K. Lee Y. (1998) “Comparative analysis of jet impingement and microchannel cooling for high heatflux applications”, International Journal of Heat and Mass,42, 444–457.

[25] Pattamata A., Siva M. (2014), “Investigation on Flow Maldistribution in Parallel Microchannel Systems For Integrated Microelectronic Device Cooling”, Ieee Transactıons On Components, Packagıng And Manufacturıng Technology 4(3), 438–450.

[26] Missaggia, L. J. (1989). “Microchannel Heat Sinks for Two-Dimensional High-Power-Density Diode Laser Arrays”, IEEE Journal Of Quantum Electronıcs, 2(9), 1988–1992.

[27] Mudawar, I. (2001). “Assessment Of High-Heat-Flux Thermal Management Scemes”, Ieee Transactıons On Components And Packagıng Technologıes 24(2), 122–141.

[28] Yadav, V., Kumar, R., & Narain, A. (2018). “Mitigation of Flow Maldistribution in Parallel Microchannel Heat Sink”. IEEE Transactions on Components, Packaging and Manufacturing Technology, PP(c),

[29] Tien, C.L., and Kuo, S.M., “Analysis of forced convection in microstructures for electronic system cooling.” In Proceedings of the International Symposium on Cooling Technology for Electronic Equipment, Honolulu, Hl, 1987, pp. 217-226

BIOGRAPHY

Ali Elmalı was born in Sivas in 12 August 1989. After he had graduated from Semiha Şakir High School in 2006, took the Bachelor's Degree from Kocali University Department of Mechanical Engineering in 2012. He started graduate school at Gebze Technical University, Graduate School of Natural and Applied Sciences Department of Mechanical Engineering. He has been working at Birgi A.S as a Production Engineer.